OAK RIDGE NATIONAL LABORATORY LIBRARIES
3 4456 0548156 4

CENTRAL RESEARCH LIBRARY
DOCUMENT COLLECTION

1

ORNL-3992
UC-25 – Metals, Ceramics, and Materials

CREEP-RUPTURE PROPERTIES OF TUNGSTEN AND TUNGSTEN-BASE ALLOYS

H. E. McCoy

CENTRAL RESEARCH LIBRARY
DOCUMENT COLLECTION
LIBRARY LOAN COPY
DO NOT TRANSFER TO ANOTHER PERSON
If you wish someone else to see this document, send in name with document and the library will arrange a loan.

OAK RIDGE NATIONAL LABORATORY
operated by
UNION CARBIDE CORPORATION
for the
U.S. ATOMIC ENERGY COMMISSION

Printed in USA. Price $3.00 . Available from the Clearinghouse for Federal Scientific and Technical Information, National Bureau of Standards, U.S. Department of Commerce, Springfield, Virginia 22151

LEGAL NOTICE

This report was prepared as an account of Government sponsored work. Neither the United States, nor the Commission, nor any person acting on behalf of the Commission:

A. Makes any warranty or representation, expressed or implied, with respect to the accuracy, completeness, or usefulness of the information contained in this report, or that the use of any information, apparatus, method, or process disclosed in this report may not infringe privately owned rights; or

B. Assumes any liabilities with respect to the use of, or for damages resulting from the use of any information, apparatus, method, or process disclosed in this report.

As used in the above, "person acting on behalf of the Commission" includes any employee or contractor of the Commission, or employee of such contractor, to the extent that such employee or contractor of the Commission, or employee of such contractor prepares, disseminates, or provides access to, any information pursuant to his employment or contract with the Commission, or his employment with such contractor.

ORNL-3992

Contract No. W-7405-eng-26

METALS AND CERAMICS DIVISION

CREEP-RUPTURE PROPERTIES OF TUNGSTEN AND TUNGSTEN-BASE ALLOYS

H. E. McCoy

AUGUST 1966

OAK RIDGE NATIONAL LABORATORY
Oak Ridge, Tennessee
operated by
UNION CARBIDE CORPORATION
for the
U.S. ATOMIC ENERGY COMMISSION

OAK RIDGE NATIONAL LABORATORY LIBRARIES

3 4456 0548156 4

CONTENTS

	Page
Abstract	1
Introduction	1
Experimental Details	2
Test Materials	2
Powder-Metallurgy Tungsten Sheet	2
Thermochemically-Deposited Tungsten	2
W–2% ThO_2 Alloy	4
Sylvania A	4
Test Specimens	4
Testing Methods	6
Experimental Findings	6
Powder-Metallurgy Tungsten	6
Thermochemically-Deposited Tungsten	16
W–2% ThO_2 Alloy	32
Sylvania A	40
Summary and Conclusions	46
Acknowledgment	48

CREEP-RUPTURE PROPERTIES OF TUNGSTEN AND TUNGSTEN-BASE ALLOYS

H. E. McCoy

ABSTRACT

The creep-rupture properties of two types of unalloyed tungsten and two tungsten-base alloys were determined at 1650 and 2200°C for times of at least 500 hr. The materials studied were wrought powder-metallurgy tungsten, several lots of thermochemically deposited (TCD) tungsten, W–2% ThO_2, and Sylvania A (W–0.5% Hf–0.02% C). At 1650°C the order of strengths from the greatest to least was W–2% ThO_2, Sylvania A, and TCD and powder-metallurgy tungsten. At 2200°C the order of strengths from greatest to least was W–2% ThO_2, TCD and powder-metallurgy tungsten, and Sylvania A. The ductility of the TCD tungsten was low at 1650°C, but was good at 2200°C. The W–2% ThO_2 showed moderate ductility at both temperatures. The ductility of the Sylvania A improved from moderate at 1650°C to good at 2200°C. The powder-metallurgy tungsten had good ductility at both test temperatures. All of the materials studied exhibited better high-temperature grain-size stability than the powder-metallurgy material. Voids formed in the TCD tungsten at 2200°C and grew to quite large sizes under an imposed stress. These voids were thought to be associated with impurities.

INTRODUCTION

Small parts have been made from tungsten for many years. However, the role of tungsten as a structural material for engineering systems is relatively new. This new interest in tungsten makes it necessary that physical and mechanical property data be obtained which are adequate for designing and constructing engineering systems. The development of tungsten-base alloys has also become active, as efforts are being made to improve the low-temperature ductility and the high-temperature creep properties of unalloyed tungsten. Each new composition must be evaluated to ascertain the degree of improvement.

The present study is concerned with the high-temperature creep properties of unalloyed tungsten and several tungsten-base alloys. A check of the literature shows that long-term (100- to 1000-hr) creep data are not available even for unalloyed tungsten. For this reason a sheet of wrought powder-metallurgy tungsten was included in this study. Several heats of thermochemically deposited (TCD) tungsten were evaluated. This material is particularly interesting because it can be deposited in the desired shape at low temperatures without subsequent fabrication. The alloys W–2 wt % ThO_2 and W–0.5% Hf–0.02% C (Sylvania A) contain a dispersed phase of thoria and hafnium carbide, respectively. This dispersion should stabilize the grain size to higher temperatures and may strengthen the material. Creep studies were carried out on these four materials at 1650°C and 2200°C to rupture times of at least 500 hr. The materials are described below, and their chemical analyses are given in Table 1. Supplementary metallographic studies were carried out on the tested specimens.

EXPERIMENTAL DETAILS

Test Materials

Powder-Metallurgy Tungsten Sheet

The tungsten sheet was obtained under a Bureau of Naval Weapons Contract and the fabrication details are covered in the final report[1] on this contract. It was fabricated by the powder-metallurgy technique and was rolled to a final thickness of 0.060 in. The final treatment was an anneal at 1150°C for 5 min.

Thermochemically-Deposited Tungsten

The TCD material was produced by the hydrogen reduction of WF_6 on a heated substrate. The details of the deposition process have been

[1]G. C. Bodine, Tungsten Sheet Rolling Program – Final Report Covering Period 1 June 1960 to 1 March 1963, Fansteel Metallurgical Corporation, under Contract No. NOW-60-0621-C (March 1, 1963).

Table 1. Chemical Analysis of Test Material

Material	Interstitial Content, wt %				
	Oxygen	Nitrogen	Hydrogen	Carbon	Other
Powder-metallurgy tungsten	0.0029	<0.0005	0.0004	<0.001	
TCD, H-16	0.0064	<0.0005	0.0005	0.002	
TCD, PW-3	0.011	<0.0005	0.0004	0.003	
TCD, PW-19	0.014	0.0009	0.0005	0.002	
TCD, PW-20	<0.0005	<0.0005	0.0001	0.003	
TCD, PW-23	0.0067	<0.0005	0.0002	0.001	
TCD, PW-24	0.022	0.0014	0.0002	0.004	
W–2% ThO_2	0.25	<0.0005	0.0001	0.0008	0.0060 Ta, <0.03 Fe, 1.72 Th
Sylvania A	0.0023	0.0007	0.0001	0.034	0.64 Hf

described previously.[2] The material was deposited as a box about 2 × 2 in. in cross section and 20 in. long. It was deposited on the inside of a mandrel – copper for the "H" series and molybdenum for the "P" series. The mandrel was removed by etching and test specimens were made from the deposited box.

W–2% ThO_2 Alloy

The tungsten-base alloy containing 2% thoria was obtained from the Wah Chang Corporation (vendor designation: lot No. T68) as 1/4-in.-diam centerless ground rod. Specimens were made from the rod by grinding. Although the history of the rod is not known, it is reasoned (based on metallographic and annealing studies) that the material had been warm worked. The rod may have been stress-relieved, but it definitely was not completely recrystallized.

Sylvania A

A small sheet of the tungsten-base alloy containing hafnium carbide was obtained from Sylvania Chemical and Metallurgical Division. The sheet was 0.040 in. thick and none of the fabrication history is known.

Test Specimens

Sheet specimens of two different geometries were used. One had a gage section 3 × 0.2 in. and an overall length of 10 in. To conserve material, a smaller specimen having a gage section 1.5 × 0.25 in. and an overall length of 3.5 in. was also used. Both specimens had holes near the end for pinning them to the extension rods. Specimens of powder-metallurgy tungsten and Sylvania A were made by grinding.

The as-deposited TCD tungsten was too fragile to be ground. The sides of each box were separated by grinding and the specimens with 1.5 × 0.25-in. gage were made by electro-discharge machining. The tool

[2]R. L. Heestand, J. I. Federer, and C. F. Leitten, Jr., Preparation and Evaluation of Vapor Deposited Tungsten, ORNL-3662 (August 1964).

shown in Fig. 1 was used in conjunction with an elox machine for this purpose. The specimen outline was "cut" by segments of brass tubing and shim stock which were held in a fixture. Thus, the tool is inexpensive and can be easily replaced when the brass pieces wear. About 0.002 in. was removed from the machined surfaces by abrasion with diamond paste to remove small intergranular cracks that were formed by the electro-discharge machining.

Small rod specimens were ground from the W–2% ThO_2 alloy. These specimens had a gage section 1 in. long and 1/8 in. in diameter. The gage section blended into the 1/4-in.-diam ends by a 3/16-in. radius. These specimens were gripped by a tungsten fixture which was slotted and had an internal surface ground to match the specimen radius.

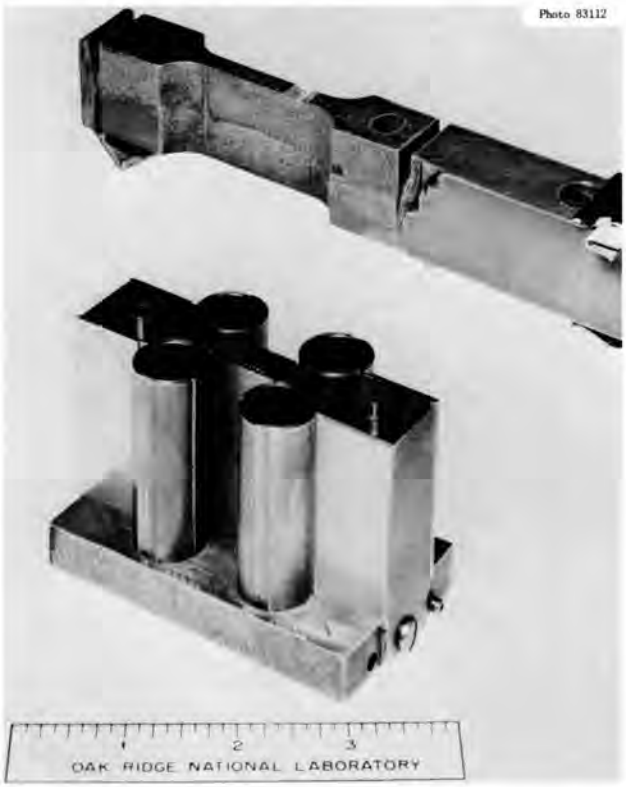

Fig. 1. Fixture Used to Make Tungsten Creep Specimens by Electro-Discharge Machining.

Testing Methods

All of the tests were run in a Brew Furnace, Model No. 1064. It has a tungsten mesh heating element and a maximum temperature capability of 2760°C. The vacuum system was cold trapped and was capable of maintaining a pressure of 1×10^{-7} torr at a test temperature of 2200°C. The temperature was controlled by a total radiation pyrometer which was sighted toward the test specimen and a controller which adjusted the power to the furnace. This control system was stated to have a control accuracy of ±3°C. The temperature could also be read by an optical pyrometer through a sight port in the front of the test chamber. The strain was measured by a dial gage which indicated the motion of the pull rod.

Test specimens were normally built into the test equipment, pumped for 2 hr, heated to about 600°C and pumped for 12 hr, heated to the test temperature in about 4 hr, and loaded.

Several specimens were analyzed for interstitials after testing. No evidence of contamination was noted except in cases where the pressure was known to have increased during the test. Data from tests where leaks were known to have developed have not been considered.

EXPERIMENTAL FINDINGS

Powder-Metallurgy Tungsten

The results of creep tests run on powder-metallurgy tungsten are summarized in Table 2. Sheet specimens of two different geometries were used. However, no effect of specimen geometry was noted and data from both designs have been used indiscriminately. Specimens were cut so that the gage length was oriented parallel (longitudinal), perpendicular (transverse), and at 45° to the rolling direction.

The data are shown graphically to illustrate several important points. Figure 2 shows the creep-rupture properties at 1650 and 2200°C. These curves are also shown in Fig. 3 where data are included for the times to 2 and 10% strain. Minimum creep rate data are shown in Fig. 4.

Table 2. Creep Properties of Powder-Metallurgy Tungsten

Test Number	Specimen		Stress (psi)	Time to Indicated Strain, hr					Rupture Strain (%)	Minimum Creep Rate (%/hr)
	Gage Length (in.)	Orientation[a]		1%	2%	5%	10%	Rupture		
				Tested at 1650°C						
3295	1 1/2	T	11,000	0.03	0.10	0.34	0.80	2.0	59.4	10.9
3356	1 1/2	T	11,000	0.05	0.08	0.6	1.6	4.85	50.0	5.2
3364	1 1/2	T	11,000	0.02	0.06	0.25	0.60	1.6	56.2	14.0
3296	1 1/2	L	10,000	0.04	0.10	0.4	1.25	4.25	50.0	6.2
3834	1 1/2	T	10,000	0.04	0.08	0.22	0.6	1.5	62.5	13.0
3294	1 1/2	L	8,000	0.2	0.5	2.5	5.8	16.1	43.7	1.5
3402	1 1/2	L	7,000	0.6	1.5	5.3	12.2	25.7	35.4	0.77
3416	1 1/2	L	7,000	0.4	1.4	5.4	15	28.35	33.3	0.63
3337	1 1/2	L	6,000	1.0	5.0	21	48	100.8	34.4	0.19
3350	1 1/2	T	6,000	2.0	8.0	31	69	133.3	31.2	0.13
3368	1 1/2	T	6,000	1.0	4.5	16.5	35.5	65.5	29.2	0.25
3523	1 1/2	45°	6,000	0.5	1.5	6.5	17	55.7	54.7	0.32
3399	1 1/2	T	4,000	35	75	170	300	568.9	39.3	0.033
				Tested at 2200°C						
2975	3	T	4,000	0.16	0.32	0.65	0.94	1.05	15.6	6.2
3004	3	L	4,000	0.2	0.5	1.0	1.4	1.8	21.9	3.8
3272	1 1/2	T	3,500	0.1	0.3	0.9	1.4	2.05	25.0	4.85
3057	3	L	2,800	2.6	4.1	4.8	5.4	6.3	21.9	0.38
3046	3	T	2,000	3.5	4.3	5.4	7.2	11.65	20.2	0.20
3045	3	L	2,000	8	11.5	13.6	18.0	32.5	29.1	0.14
3677	1 1/2	L	1,500	2.5	6	18	37	42.1	16.6	0.20
3839	1 1/2	45°	1,400	4.5	16	70		100.9	8.6	0.043
3832	1 1/2	L	1,400	1.0	8	45	97	122.6	16.7	0.080
3833	1 1/2	T	1,400	4.0	9	15	19	42.8	29.2	0.22
3490	1 1/2	T	1,000	10	25	225		711.4	10.4	0.0070

[a](T) Transverse (L) Longitudinal

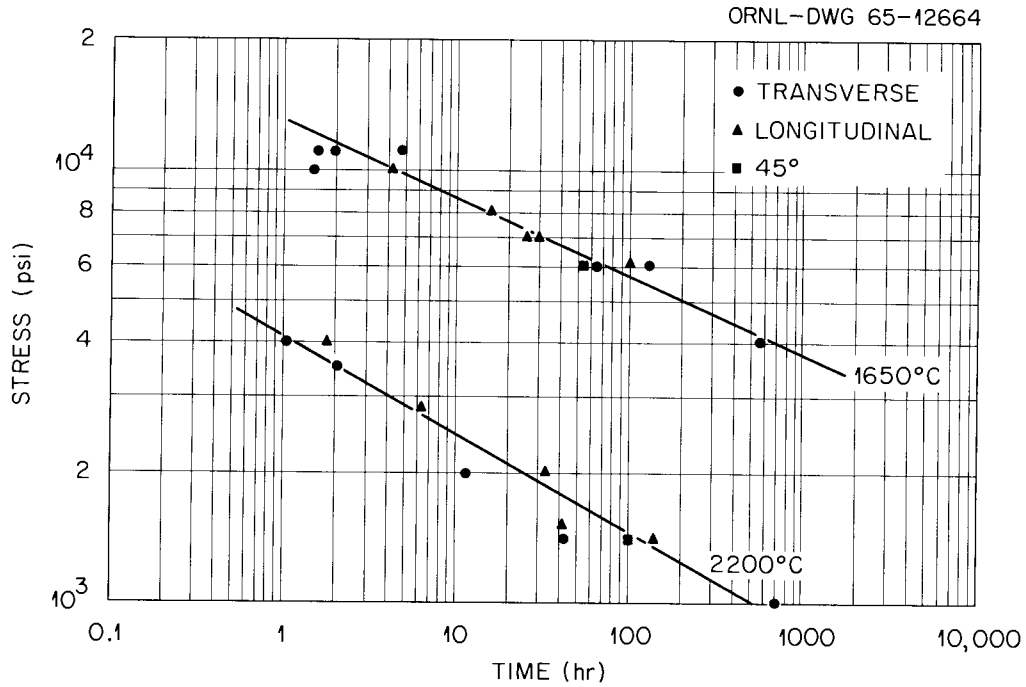

Fig. 2. Creep-Rupture Properties of Powder-Metallurgy Tungsten.

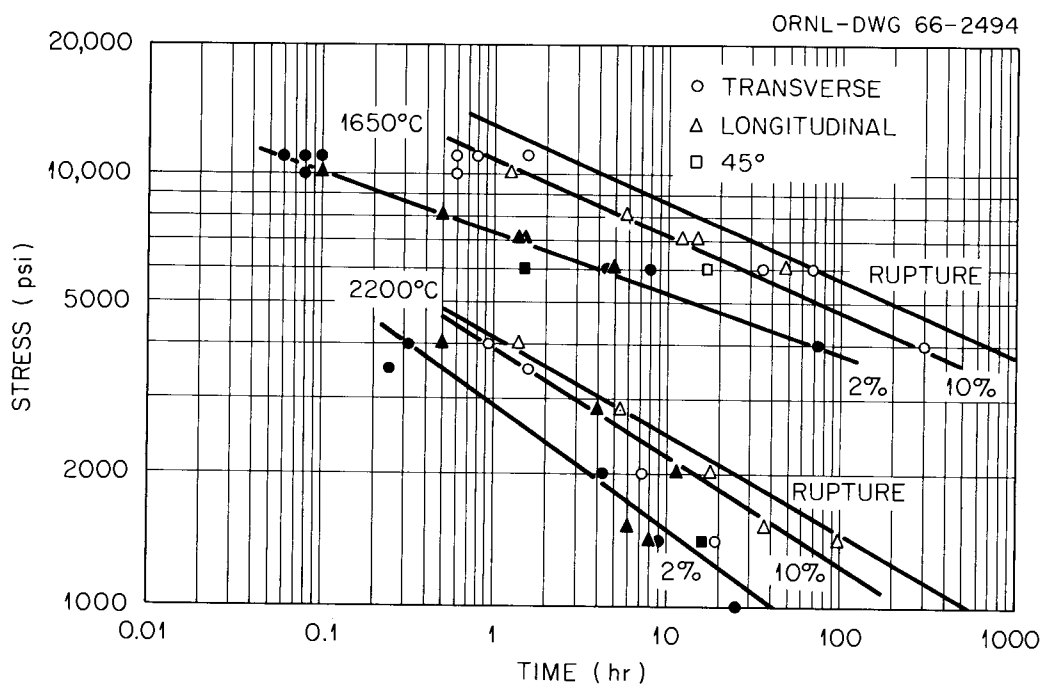

Fig. 3. Creep-Rupture Properties of Powder-Metallurgy Tungsten.

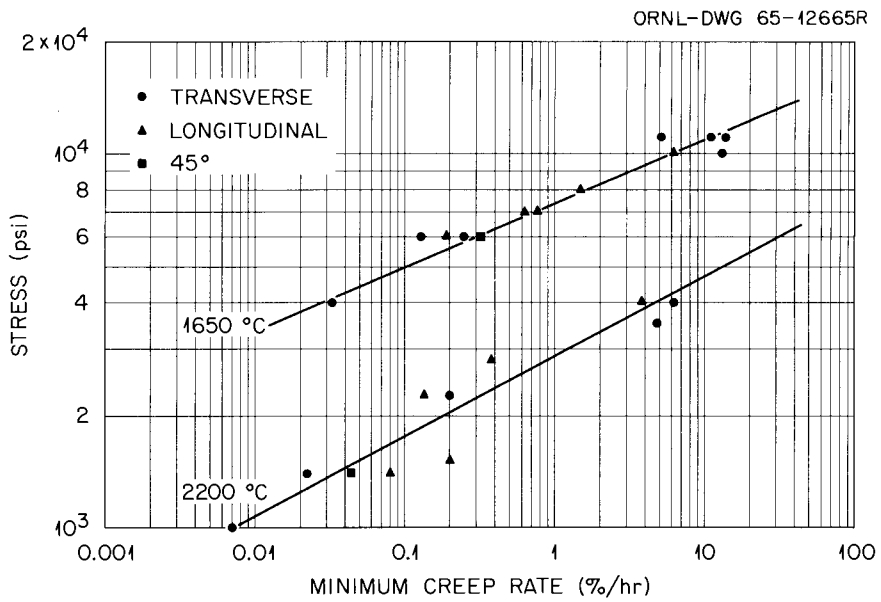

Fig. 4. Correlation of Stress and Minimum Creep Rate for Powder-Metallurgy Tungsten.

The scatter of the data is quite apparent in Figs. 2–4. Two factors are thought to account for this scatter. First, the material was found to deform quite inhomogeneously along the gage length. This probably reflects either chemical or working gradients. These inhomogeneities may vary from specimen to specimen and would result in scatter in the test results. A second factor is temperature variations between tests or during a test. Fogging of any of the lenses in the radiation control system as well as surface emissivity changes would result in temperature variations.

A plot of the creep-rupture life and the minimum creep rate is shown in Fig. 5. The correlation is quite good. Although the data at each temperature fall on a different line, the slope of each line equals one. This may be expressed also by the equation

$$\dot{\epsilon} t_r = \text{constant}$$

where

t_r = the rupture life,

$\dot{\epsilon}$ = the minimum creep rate.

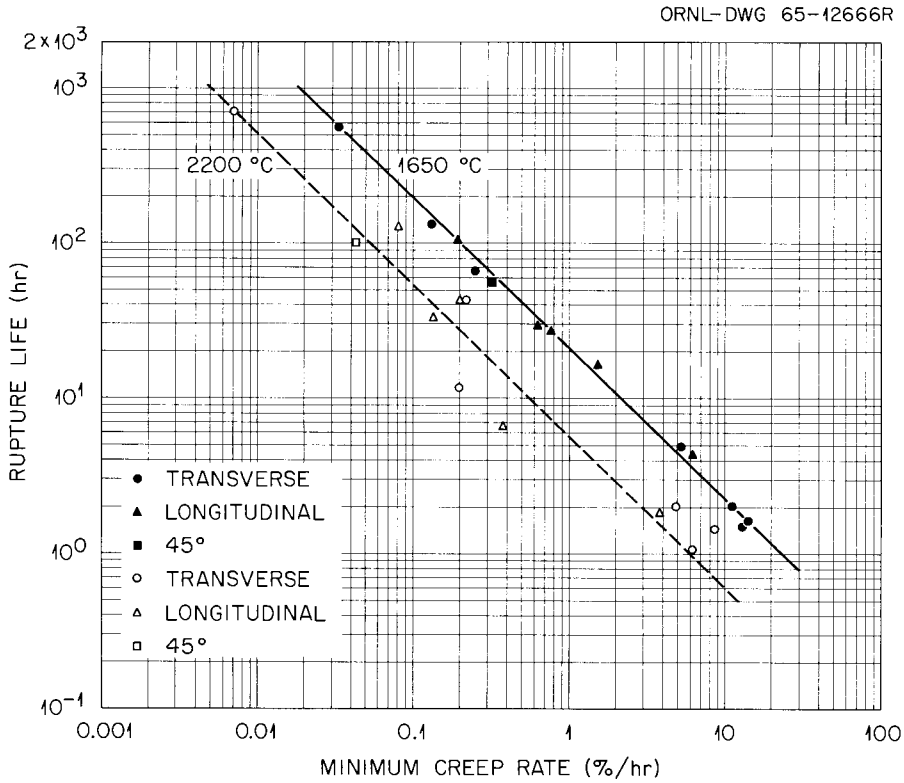

Fig. 5. Correlation of Minimum Creep Rate and Rupture Life for Powder-Metallurgy Tungsten.

Machlin[3] predicted that this equation should be obeyed for cases of intergranular fracture where the measured creep rate and the creep rate producing vacancies for voids are the same. Other investigators have shown the relationship to hold for several nickel-base alloys,[4] tungsten[5]

---

[3]E. S. Machlin, "Creep-Rupture by Vacancy Condensation," Trans. AIME 206, 106 (1956).

[4]H. E. McCoy, Effects of Hydrogen on the High-Temperature Flow and Fracture Characteristics of Metals, ORNL-3600 (June 1964).

[5]W. D. Klopp and P. L. Raffo, Effects of Purity and Structure on Recrystallization, Grain Growth, Ductility, Tensile, and Creep Properties of Arc-Melted Tungsten, NASA TN D-2503, p. 34 (November 1964).

and molybdenum,[6] and copper.[7] Monkman and Grant[8] found the general expression to apply to several materials including aluminum, titanium, austenitic and ferritic steels, and several nickel-base alloys with the slope varying from 0.77 to 0.93 rather than 1. Workers at General Electric[9] found several refractory alloys to be represented by this expression with the slope ranging from 0.94 to 0.99. Rhenium and alloys containing rhenium were notable exceptions with the slope deviating significantly from unity. The good correlation of the present data illustrates the potential use of such correlations for predicting the rupture life if only the minimum creep rate is known. If the slope of unity is assumed, only one test must be run to locate the curve.

The fracture ductilities at 1650 and 2200°C are shown in Figs. 6 and 7, respectively. The significance of the slight increase in rupture ductility with rupture life at 1650°C is not known. No significant microstructural changes were observed which might explain this behavior. At 2200°C (Fig. 7) the ductility showed a continual decrease with increasing rupture life. This is felt to be due to the excessive grain growth that occurred at this temperature.

The creep-rupture data obtained at 1650 and 2200°C in this study are compared with those of other experimenters[10,11,12] in Fig. 8.

---

[6]J. A. Houck, Physical and Mechanical Properties of Commercial Molybdenum-Base Alloys, Report 140, Defense Metals Information Center, (Nov. 30, 1960).

[7]P. Feltham and J. D. Meakin, "Creep in Face-Centered Cubic Metals with Special Reference to Copper," Acta Met. 7(9), 614 (1959).

[8]F. C. Monkman and N. J. Grant, "An Empirical Relationship Between Rupture Life and Minimum Creep Rate in Creep-Rupture Tests," Am. Soc. Testing Mater. Proc. 56, 593 (1956).

[9]Third Annual Report — High-Temperature Materials and Reactor Component Development Programs, Vol. I Materials, GEMP-270A, p. 33, (February 1964).

[10]Heinz G. Sell, et al., "Physical Metallurgy of Tungsten and Tungsten-Base Alloys," WADD TR 60-37, Part II (May 1961).

[11]W. V. Green, "Short-Time Creep-Rupture Behavior of Tungsten at 2250°C," Trans. AIME 215 (1959).

[12]Fourth Annual Report — High-Temperature Materials and Reactor Component Development Programs, Vol. I Materials, GEMP-334A, p. 33 (February 1965).

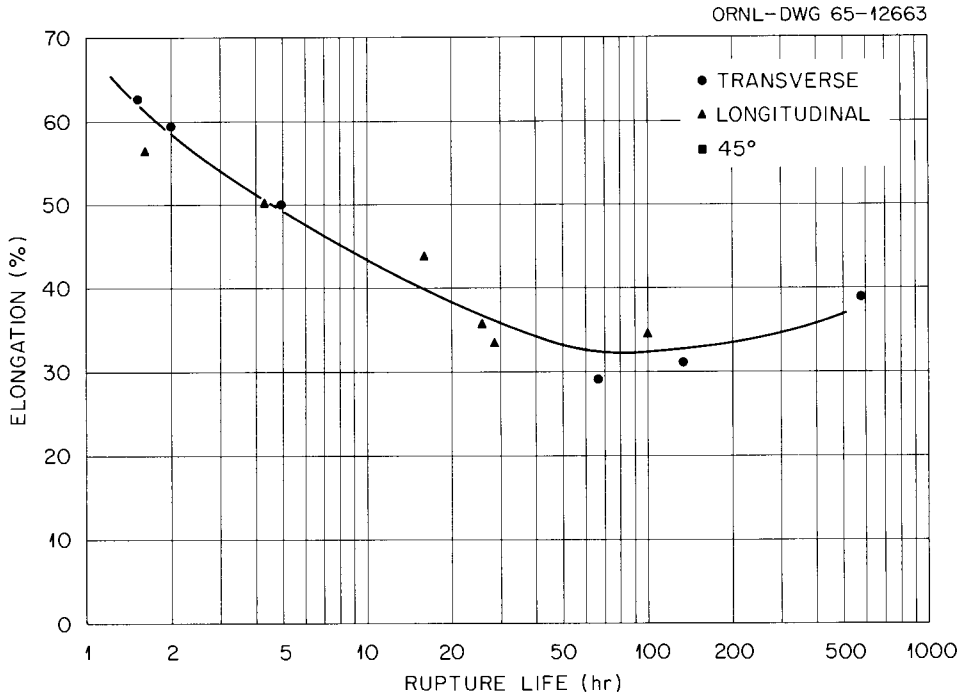

Fig. 6. Fracture Ductility of Powder-Metallurgy Tungsten at 1650°C.

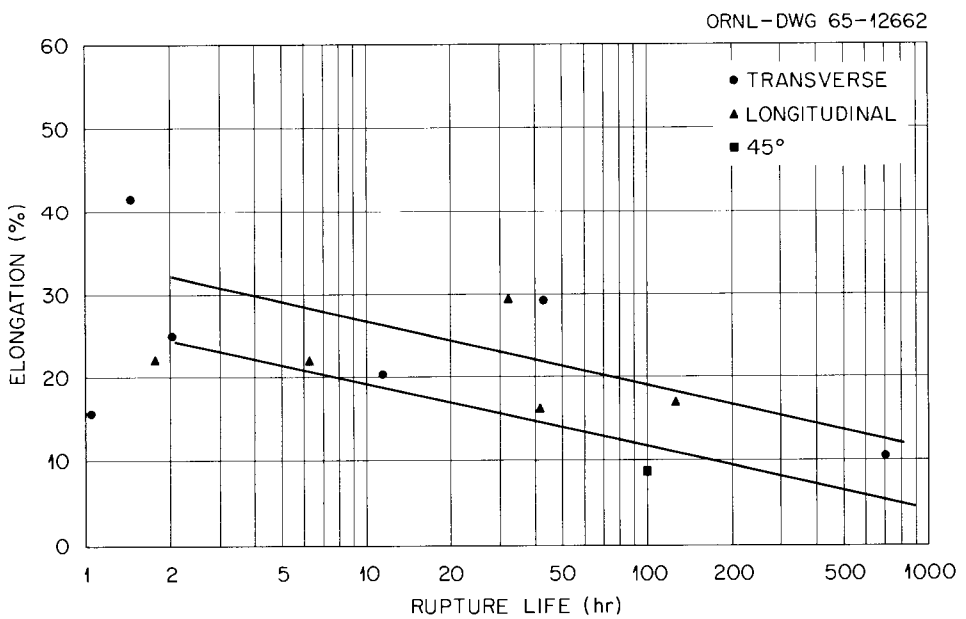

Fig. 7. Fracture Ductility of Powder-Metallurgy Tungsten at 2200°C.

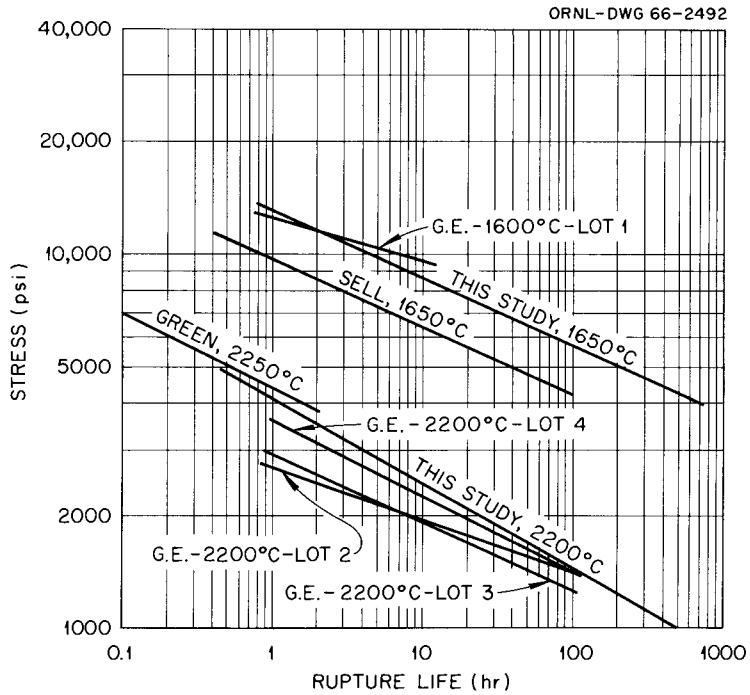

Fig. 8. A Comparison of the Creep-Rupture Properties of Tungsten.

The agreement is reasonably good, considering the fact that the material was obtained from various sources and was tested by several experimenters.

Several of the test specimens were examined metallographically. Figure 9 shows the microstructure of the as-received material. Figure 10 shows the fracture of a specimen tested at 1650°C and 6000 psi. An extensive network of intergranular cracks was formed with fracture resulting from the joining of these cracks. Figure 11 shows that some grain growth occurred in the specimens tested at 1650°C and 4000 psi. Specimens tested at 2200°C for short periods of time look very similar to those shown in Figs. 10 and 11. However, specimens tested at stresses which resulted in rupture lives greater than about 10 hr exhibited excessive grain growth. Figure 12 shows a typical area in a specimen that failed in 42.1 hr. This increase in grain size is felt to be responsible for the reduction in fracture ductility with increasing rupture life at 2200°C (Fig. 7).

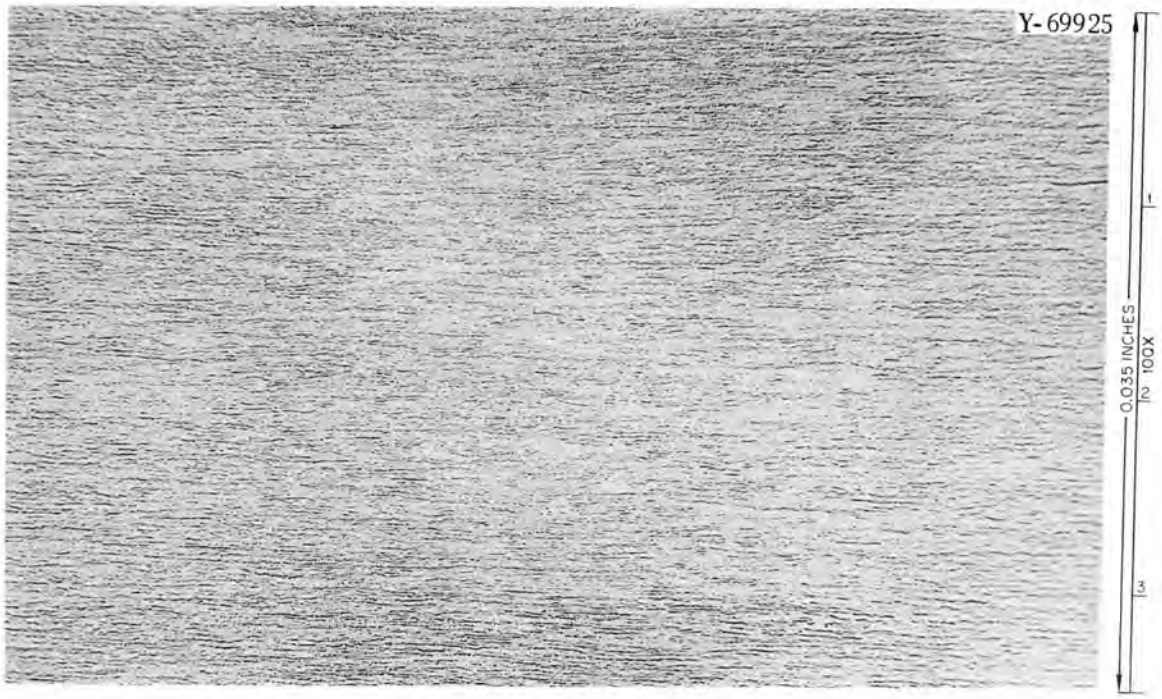

Fig. 9. Photomicrograph of Powder-Metallurgy Tungsten Sheet in the As-Received Condition. Etchant: 50 parts NH_4OH and 50 parts H_2O_2.

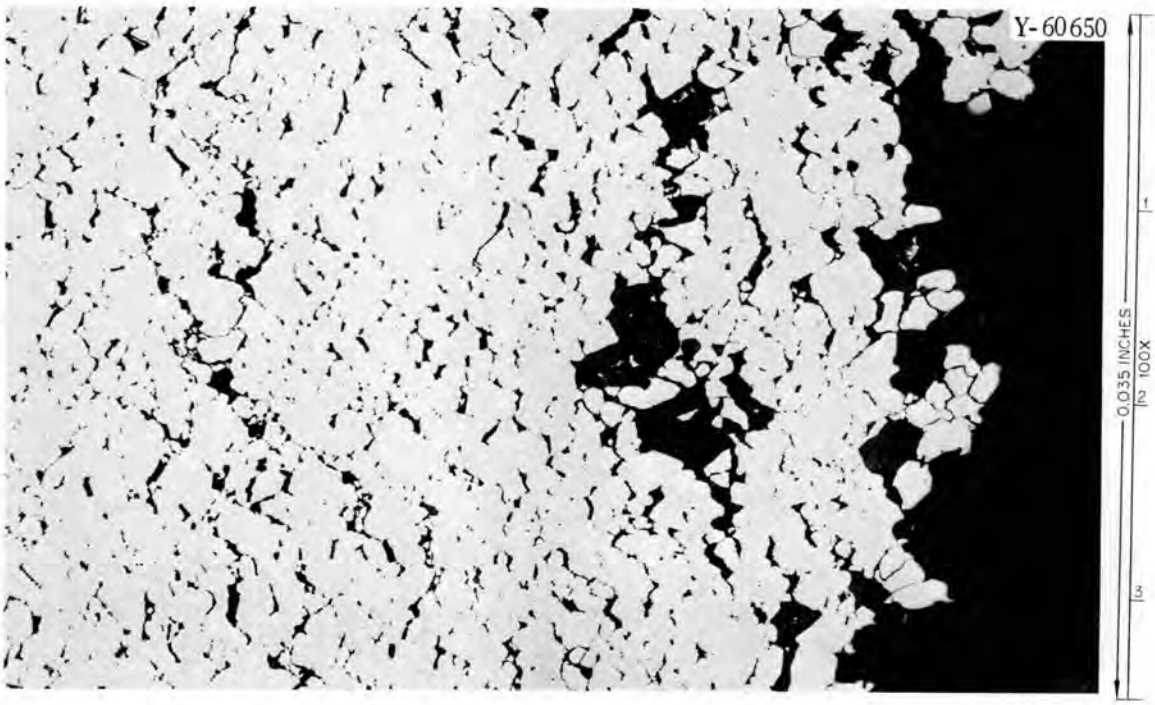

Fig. 10. Photomicrograph of Powder-Metallurgy Tungsten Sheet Tested at 6000 psi and 1650°C. Rupture occurred at 135 hr and 31.2% strain. As polished.

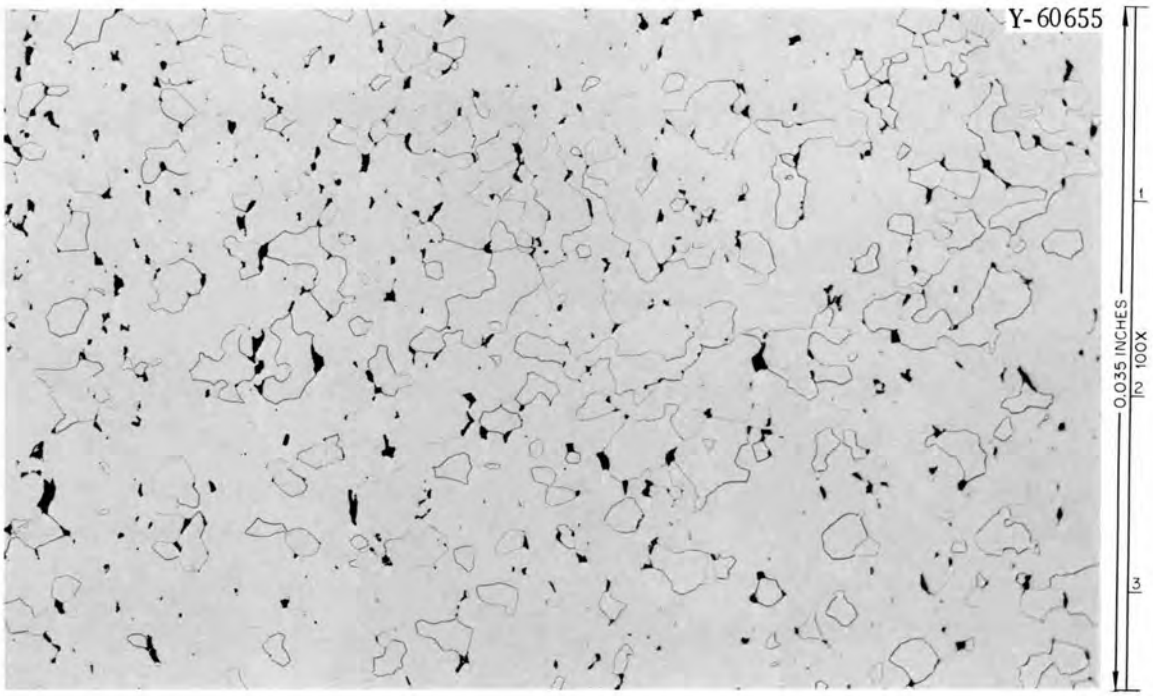

Fig. 11. Photomicrograph of Powder-Metallurgy Tungsten Sheet Tested at 4000 psi and 1650°C Rupture occurred at 568.9 hr and 39.3% Strain. Etchant: 50 parts NH_4OH and 50 parts H_2O_2.

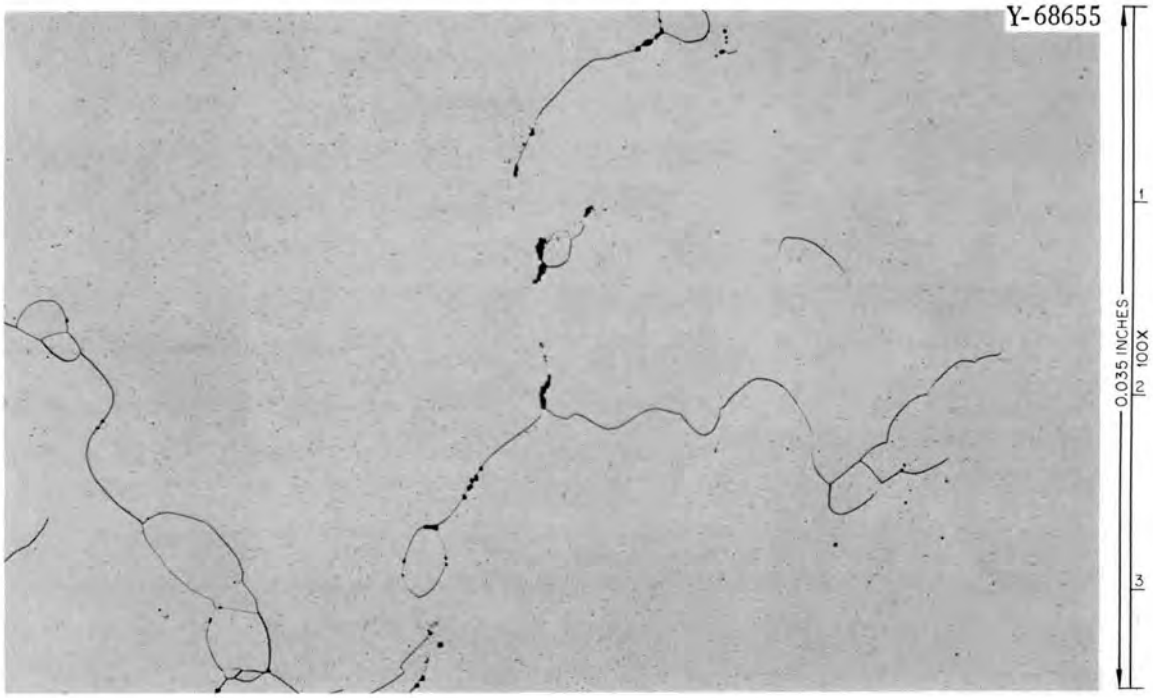

Fig. 12. Photomicrograph of Powder-Metallurgy Tungsten Tested at 1500 psi and 2200°C. Rupture occurred at 42.1 hr and 16.6% strain. Etchant: 50 parts NH_4OH and 50 parts H_2O_2.

Thermochemically Deposited Tungsten

The TCD tungsten is characterized by large columnar grains which are oriented in the thickness dimension of the deposited sheet. A layer of small grains forms at the substrate surface where the deposit begins. A cross-sectional view of a TCD sheet is shown in Fig. 13a. This particular sheet is atypical in that the gas supply was interrupted and a laminate formed near the center. A view of the sheet parallel to the surface is shown in Fig. 13b. The microstructure in this plane gives the appearance of an equiaxial grain structure. The specimens were oriented so that the stress was applied perpendicular to the columnar grain boundaries.

Several lots of TCD tungsten were studied and only a limited amount of data was obtained on each lot. For this reason the TCD tungsten results will be considered on a comparative basis with the results obtained on the powder-metallurgy tungsten. The results of the creep-rupture studies on TCD tungsten are summarized in Table 3. The creep-rupture properties of the TCD tungsten are compared with those of the powder-metallurgy tungsten in Fig. 14. Although there is some scatter, the data fall in a reasonable band about the line representing the properties of the powder-metallurgy tungsten. Figure 15 shows a comparison of the minimum creep rate of TCD and powder-metallurgy tungsten. The minimum creep rate of the TCD tungsten is less at 1650°C and greater at 2200°C. Figure 16 is a plot of the rupture life as a function of minimum creep rate. For a given creep rate, the rupture life of the TCD tungsten is less at 1650°C and greater at 2200°C as compared with that for powder-metallurgy tungsten.

Figure 17 compares the rupture ductilities of the two types of material. At 1650°C the TCD tungsten, with only one exception, has a ductility of 5% or less. At 2200°C the TCD tungsten shows a trend of increasing fracture ductility with increasing rupture life. Although the elongation at 2200°C appeared to be reasonably high, it is questionable whether this elongation is useful in the engineering sense. The reduction in area at the fracture was only a few percent. Hence, much of the elongation is probably due to the growth of the voids

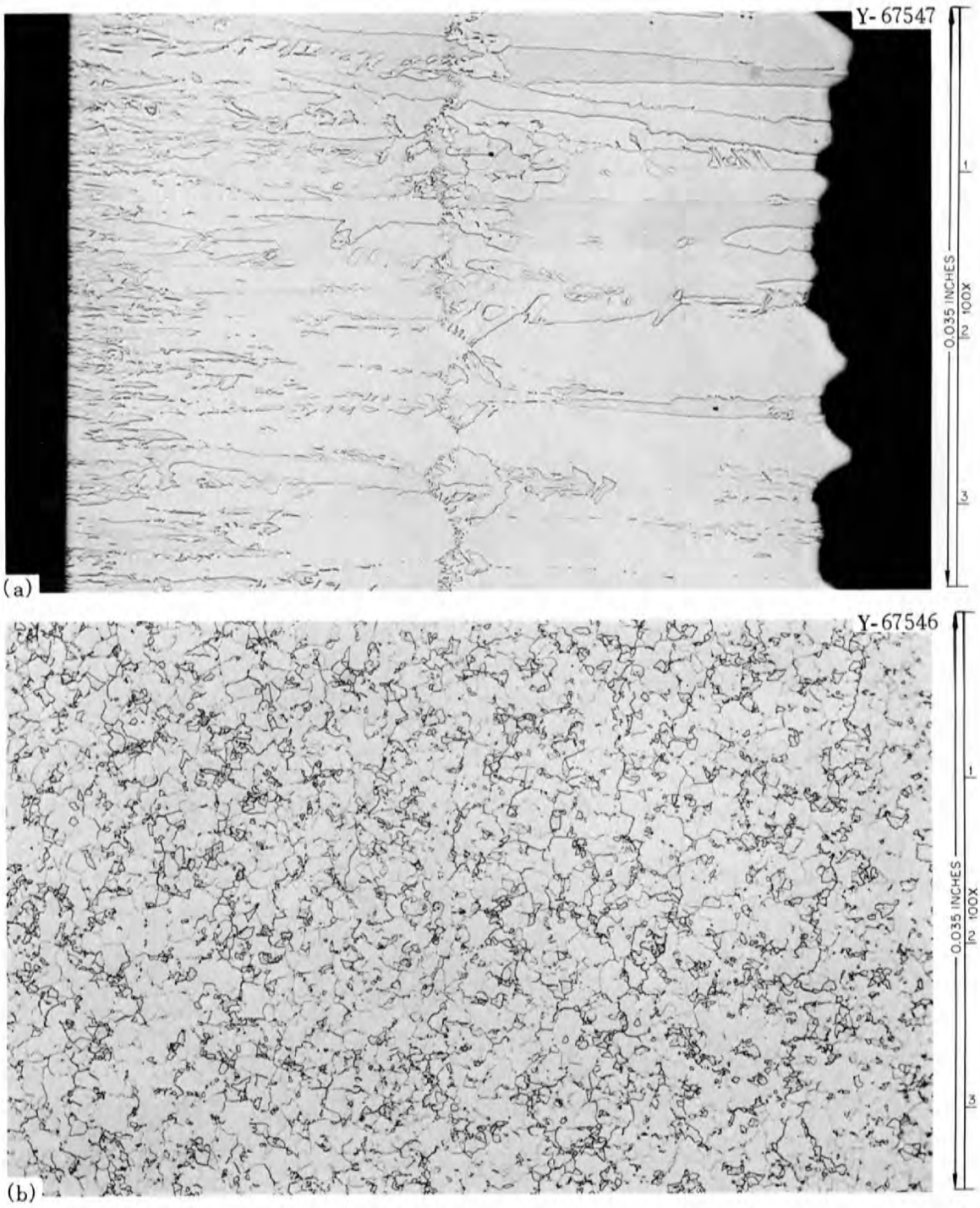

Fig. 13. Photomicrographs of As-Deposited TCD Tungsten, Lot PW-3. Etchant: 50 parts NH_4OH and 50 parts H_2O_2. (a) Cross section. (b) Parallel to surface.

Table 3. Creep-Rupture Properties of TCD Tungsten Sheet

Test Number	Lot Number	Surface Treatment	Stress (psi)	Time to Indicated Strain, hr					Rupture Strain (%)	Minimum Creep Rate (%/hr)
				1%	2%	5%	10%	Rupture		
				Tested at 1650°C						
3478	H-16	Lapped	6000	7.4	19.2			30.5	4.2	0.063
3518	H-16	Lapped	4000	5.0	35	185	390	593.7	21.0	0.020
3556	PW-3	None	6000	7.3				9.7	6.3	0.083
3837	PW-3	None	6000	4.7	11.0			12.8	3.1	0.12
3838	PW-3	None	5000	35	102			176.5	3.5	0.016
3569	PW-3	Lapped	4000	20	225			413.0	3.2	0.0040
				Tested at 2200°C						
4045	H-16	Lapped	1346	1.0	2.7	6.5	13.0	62.9	35.0	0.75
3577	PW-3	Lapped	2000	0.5	1.4	4.6	10.3	21.3	21.9	1.1
3680	PW-3	None	1500	4.7	9.3	18.0	29.3	35.7	16.6	0.19
3644	PW-3	Lapped	1250	4.0	48	160	306	789.9	29.2	0.026
4071	PW-19	None	2000	0.7	2.0			4.3	4.2	0.77
5292	PW-20	Lapped	2000	0.4	0.6	1.0	1.6	1.85	15.6	2.8
5295	PW-23	Lapped	2000	1.0	1.5	2.4	3.7	5.05	21.8	1.0
5301	PW-23	None[a]	2000	1.2	2.1	3.15	4.4	5.3	21.9	0.85
5294	PW-24	Lapped	2000	0.5	1.4	2.3	3.1	4.65	21.6	1.33

[a]Annealed 90 hr at 1650°C prior to loading.

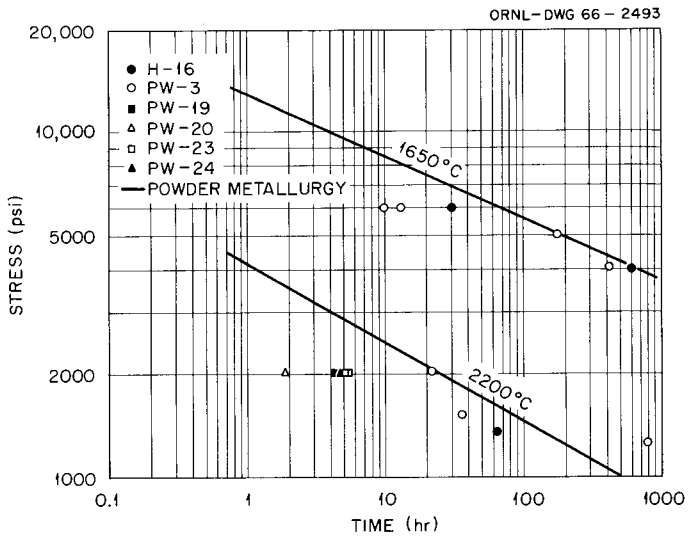

Fig. 14. Comparison of the Creep-Rupture Properties of TCD and Powder-Metallurgy Tungsten.

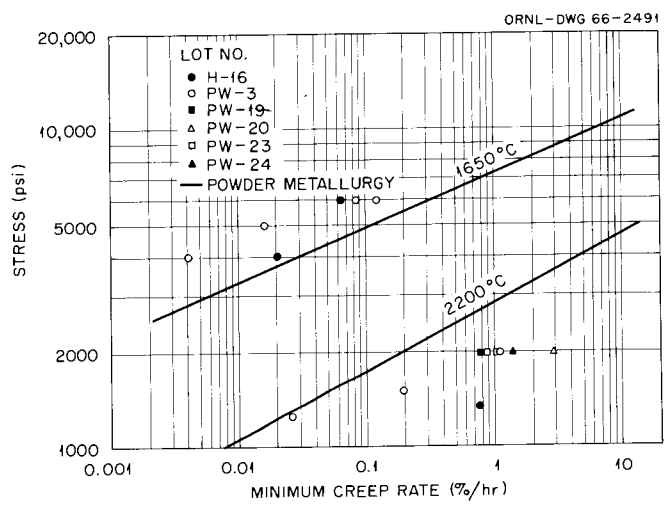

Fig. 15. Comparison of the Minimum Creep Rates of TCD and Powder-Metallurgy Tungsten.

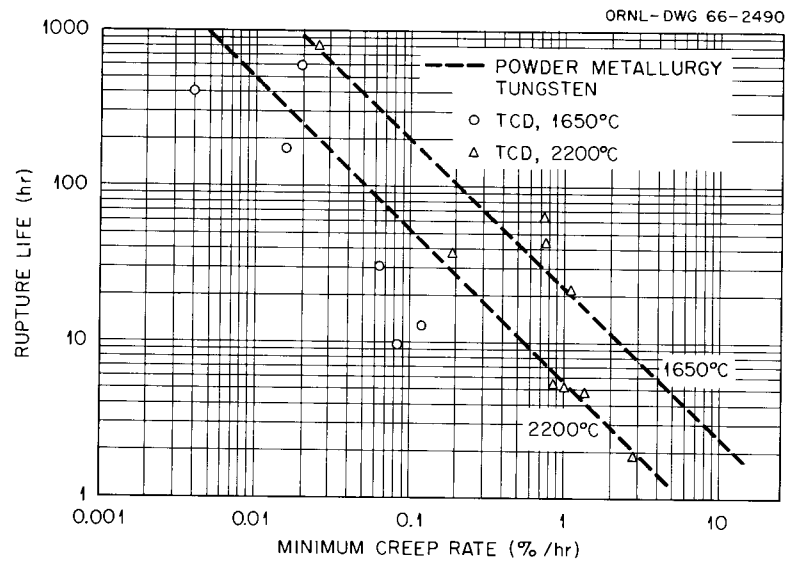

Fig. 16. Comparison of the Rupture Life and Minimum Creep Rate for TCD Tungsten.

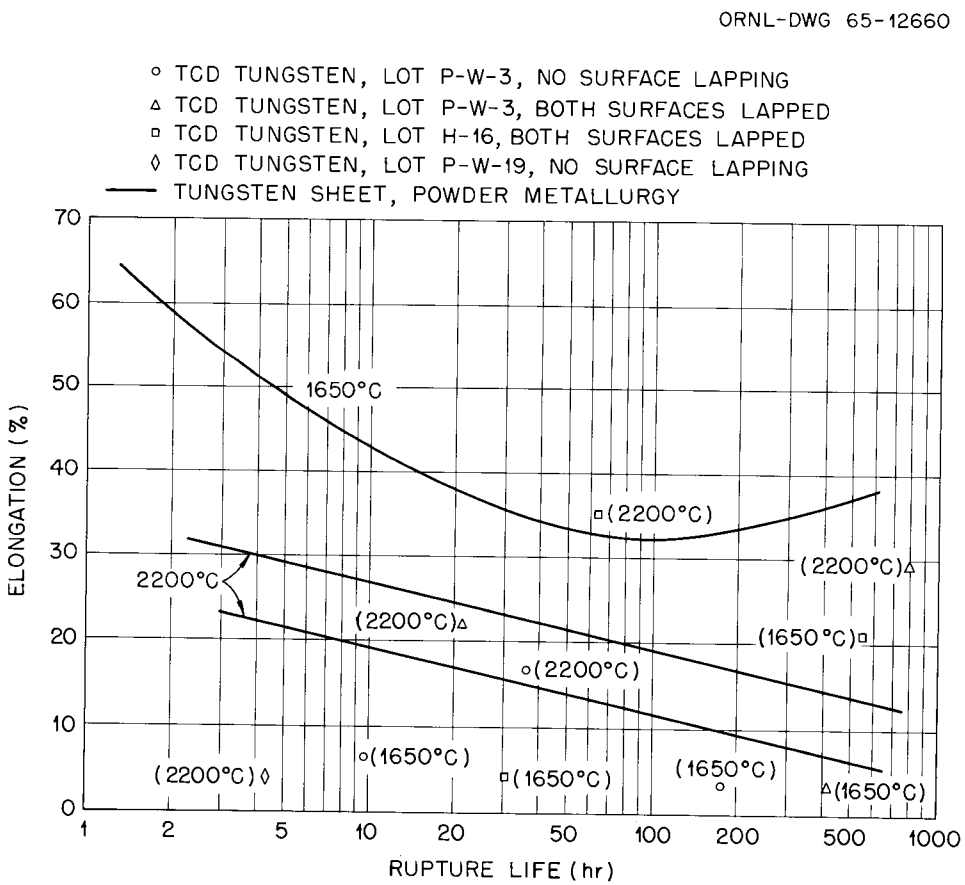

Fig. 17. Comparison of the Fracture Ductilities of TCD and Powder-Metallurgy Tungsten.

and hence does not represent plastic deformation. The matter of ductility will be discussed in more detail later.

Although some of the specimens were surface lapped to remove the first-deposited fine-grained layer and others were tested in the as-deposited condition, there appears to be no influence of this variable on any property measured.

Several of the test specimens were examined metallographically after testing. Figure 18 shows the microstructure of a specimen from lot H-16 which was tested at 6000 psi and 1650°C. Void formation was extensive throughout the specimen. Figure 18a shows the voids away from the fracture in the plane of the sheet and Fig. 18b shows that these voids are associated with the grain boundaries. A photomicrograph of a specimen from lot H-16 that was tested at 4000 psi and 1650°C is shown in Fig. 19. The voids have coalesced and grown during the 593.7-hr duration of this test. It may be significant that this is the only TCD specimen tested at 1650°C that showed high rupture ductility. It also shows a much higher volume fraction of voids than any other heat of material tested at 1650°C.

The fracture of a specimen of TCD tungsten from lot PW-3 is shown in Fig. 20a. This specimen was tested at 1650°C and 6000 psi and failed after 12.8 hr. Although the void content is reasonably high near the fracture, it is quite low away from the fracture. Figure 20b shows a view of the cross section about 1/2 in. from the fracture. Figure 21 shows a specimen of lot PW-3 that was tested at 4000 psi and 1650°C. Significant voids were again formed only near the fracture during the 413.0-hr rupture life.

Figure 22 shows the microstructure of a specimen tested at 2200°C and 2000 psi. The specimen ruptured after 21.3 hr with 21.9% strain. A general network of voids was formed. Figure 23 shows a specimen tested at 2200°C and 1250 psi. Failure occurred in 789.9 hr with 29.2% strain. Coalescence and growth of the voids have occurred so that the voids are now as large as 0.005 in. in diameter. The grain structure has also changed from the characteristically columnar grains to an equiaxial grain structure. It is felt that the formation of the equiaxial grain structure is responsible for the increase in rupture ductility with increasing rupture life at 2200°C.

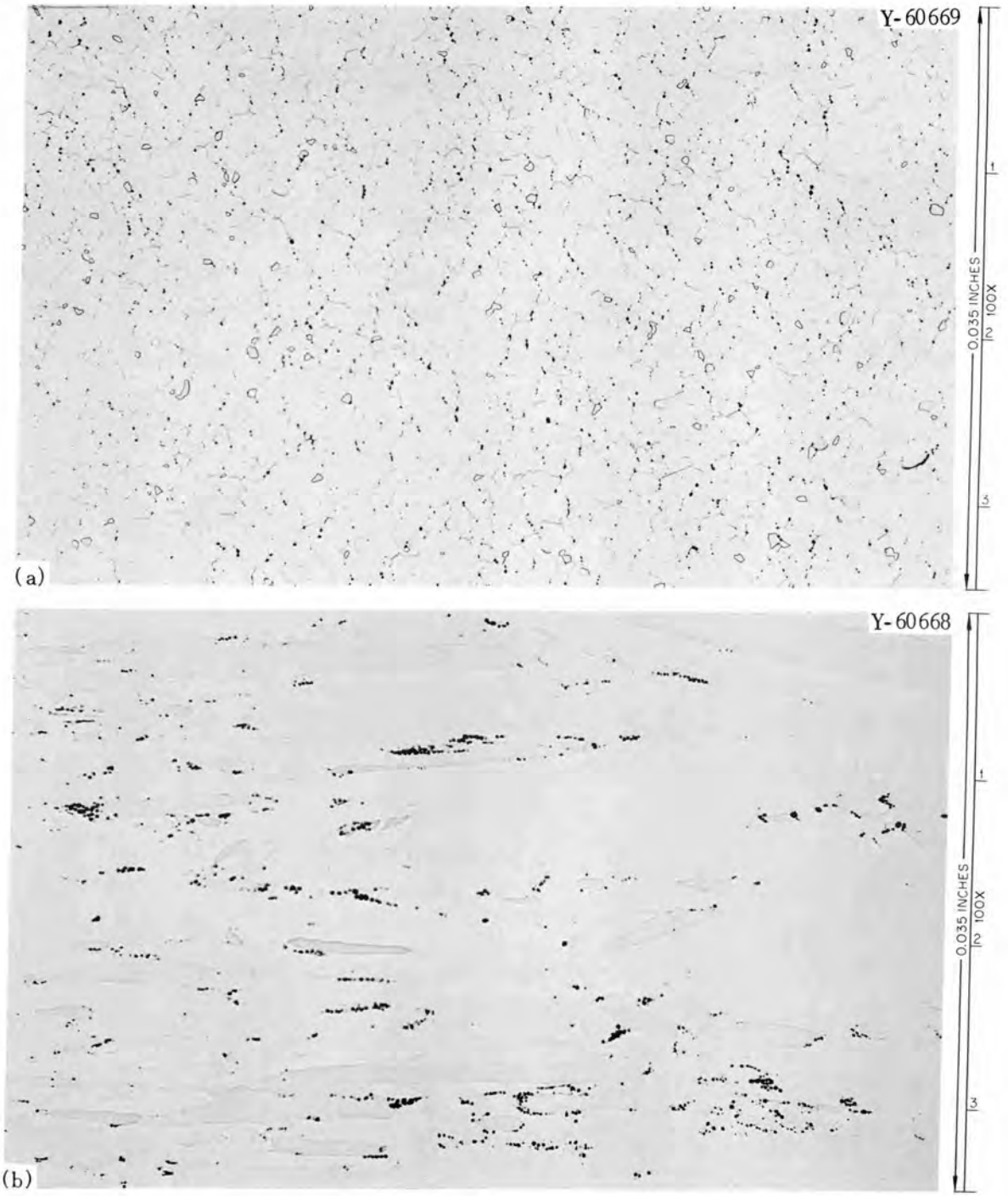

Fig. 18. Photomicrographs of a TCD Tungsten Specimen from Lot H-16 Tested at 1650°C and 6000 psi. Rupture was in 30.5 hr with 4.2% strain. Photomicrographs away from fracture. (a) Parallel to surface. (b) Cross section as polished. Etchant: 50 parts NH_4OH and 50 parts H_2O_2.

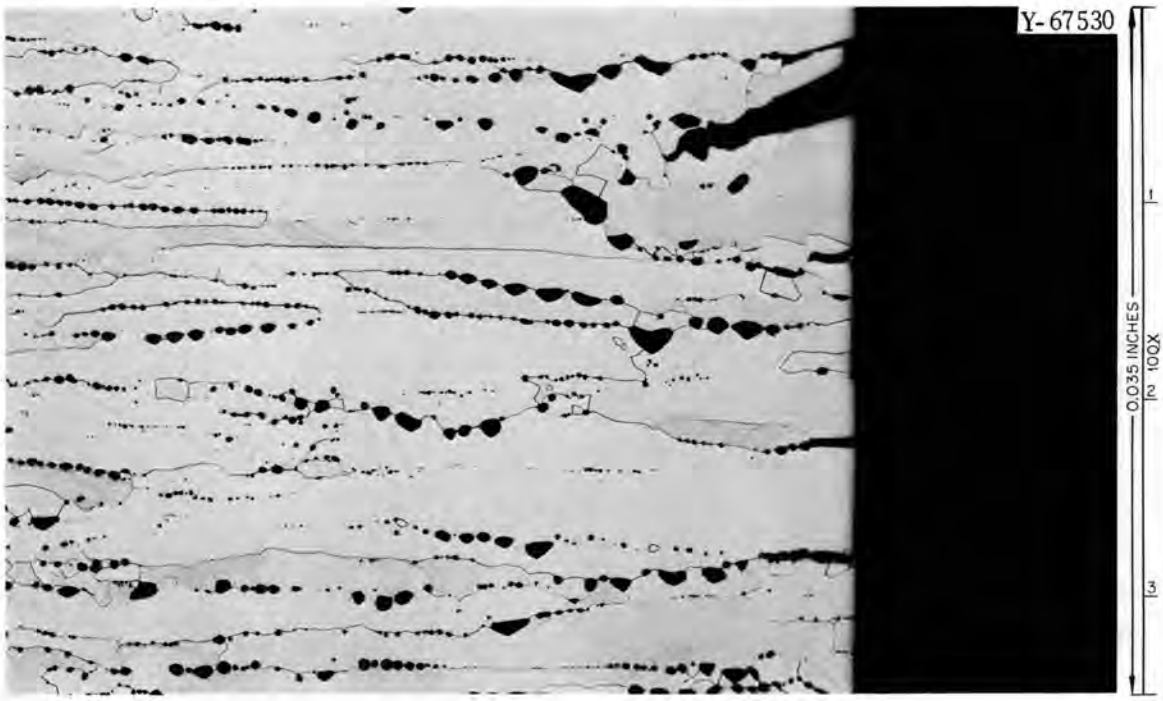

Fig. 19. Photomicrograph of the Cross Section of a TCD Tungsten Specimen from Lot H-16 Tested at 4000 psi and 1650°C. Failed in 593.7 hr with 21.0% strain. Etchant: 50 parts NH_4OH and 50 parts H_2O_2.

Figure 24 shows a specimen of TCD tungsten from lot PW-19 that was tested at 2000 psi and 2200°C. Figures 25, 26, and 27 show photomicrographs of specimens from lots PW-20, -23, and -24, respectively, that were tested at 2000 psi and 2200°C. All of these specimens show the same general microstructure with extensive void formation. Figure 28 shows a specimen of lot PW-23 that was annealed 90 hr at 1650°C prior to testing at 2000 psi and 2200°C. The void density in this specimen is quite similar to that shown in Fig. 27 for the same lot of material tested without the 1650°C anneal.

The influence of stress on the growth of the voids is demonstrated by Fig. 29 which shows the microstructure of lot PW-19 after a 5.3-hr anneal at 2200°C. This period of time is comparable with the test times for the specimens in Figs. 24, 25, 26, and 27. Although it is impossible to conclude that the number of voids is different in stressed and unstressed specimens, it is apparent that the growth of the voids is enchanced by stress.

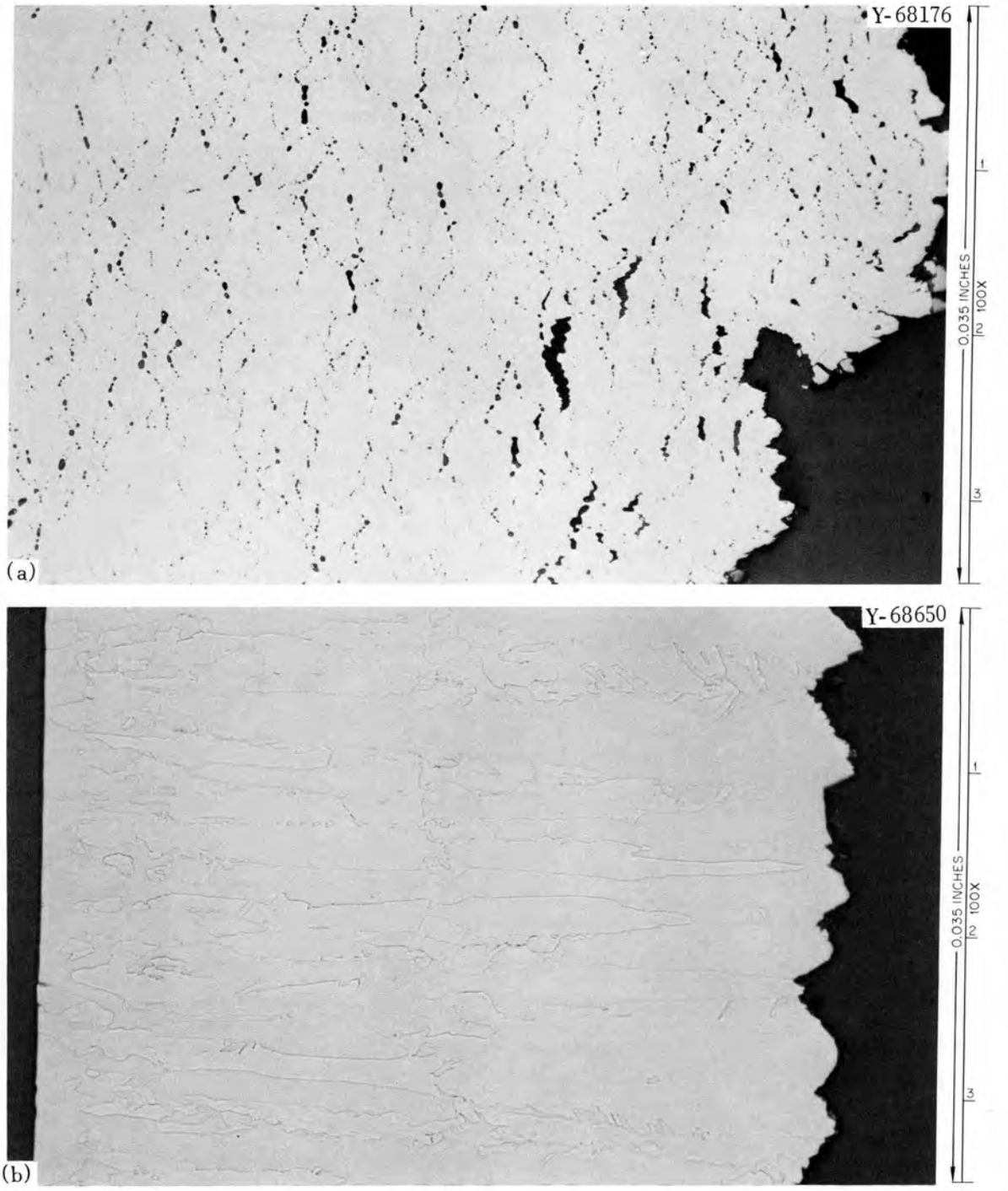

Fig. 20. Photomicrographs of TCD Tungsten from Lot PW-3 Tested at 6000 psi and 1650°C. Failure occurred in 12.8 hr and 3.1% strain. (a) Fracture, as-polished. (b) Cross section about 1/2 in. from fracture. Etchant: 50 parts NH_4OH and 50 parts H_2O_2.

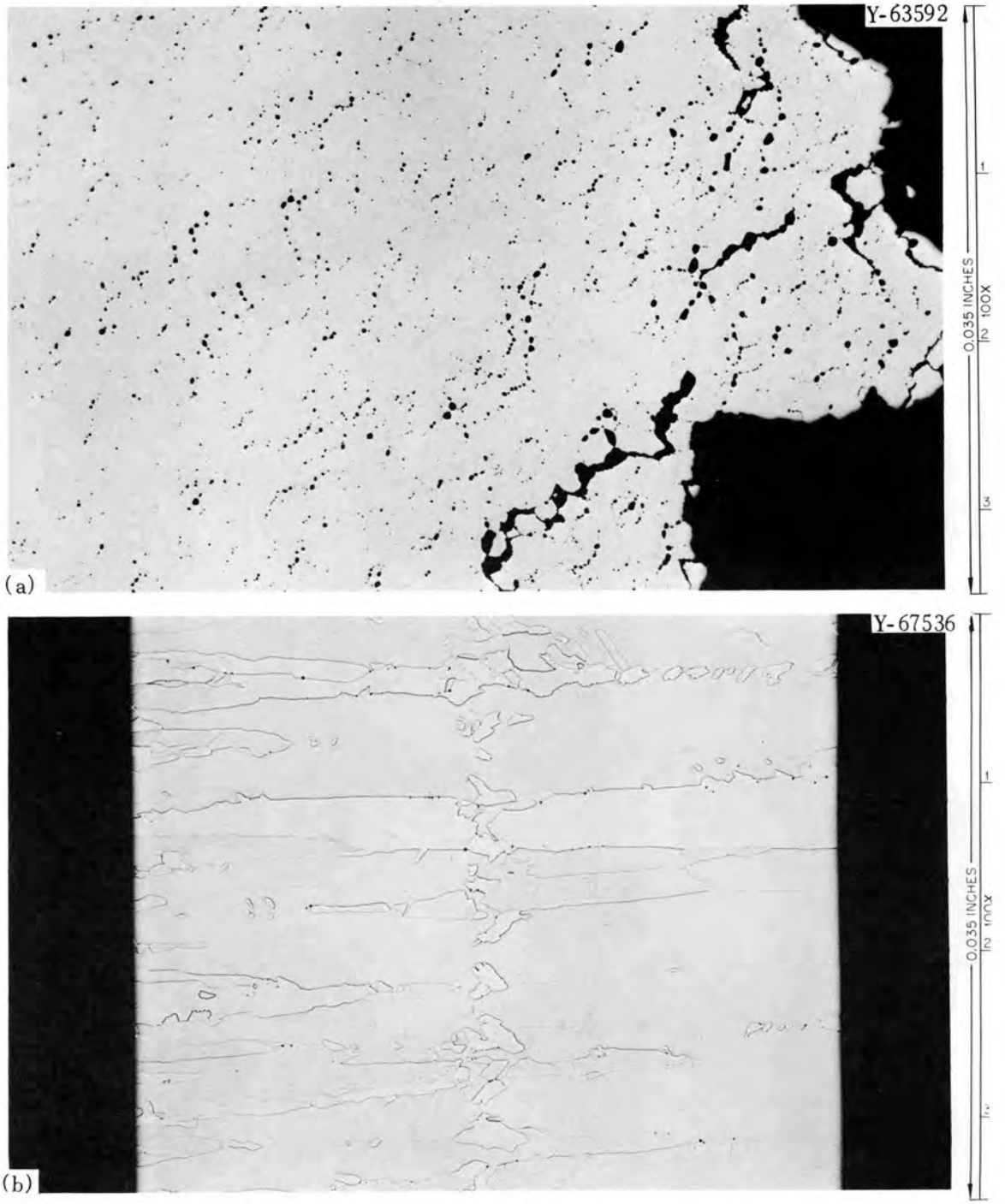

Fig. 21. Photomicrographs of TCD Tungsten from Lot PW-3, Tested at 4000 psi and 1650°C. Failed in 413.0 hr and 3.2% strain. (a) Fracture, as polished. (b) Cross section 1/2 in. from fracture. Etchant: 50 parts NH_4OH and 50 parts H_2O_2.

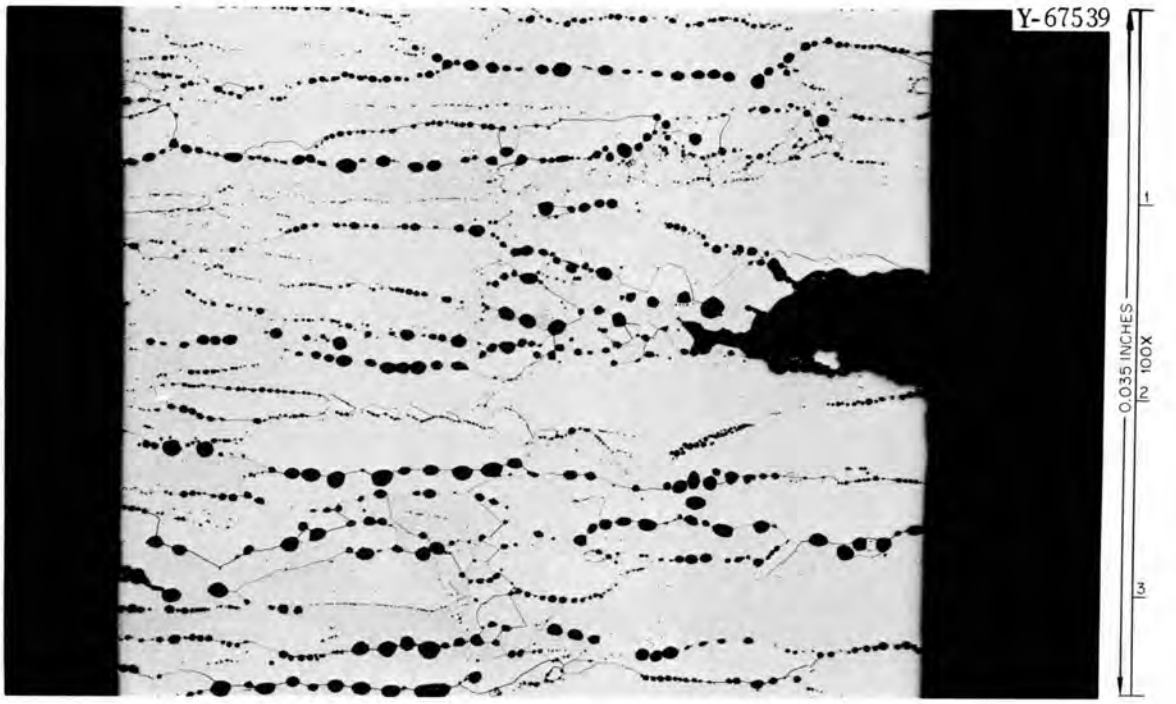

Fig. 22. Cross Section of TCD Tungsten from Lot PW-3, Tested at 2000 psi and 2200°C. Failed at 21.3 hr and 21.3% strain. Etchant: 50 parts NH_4OH and 50 parts H_2O_2.

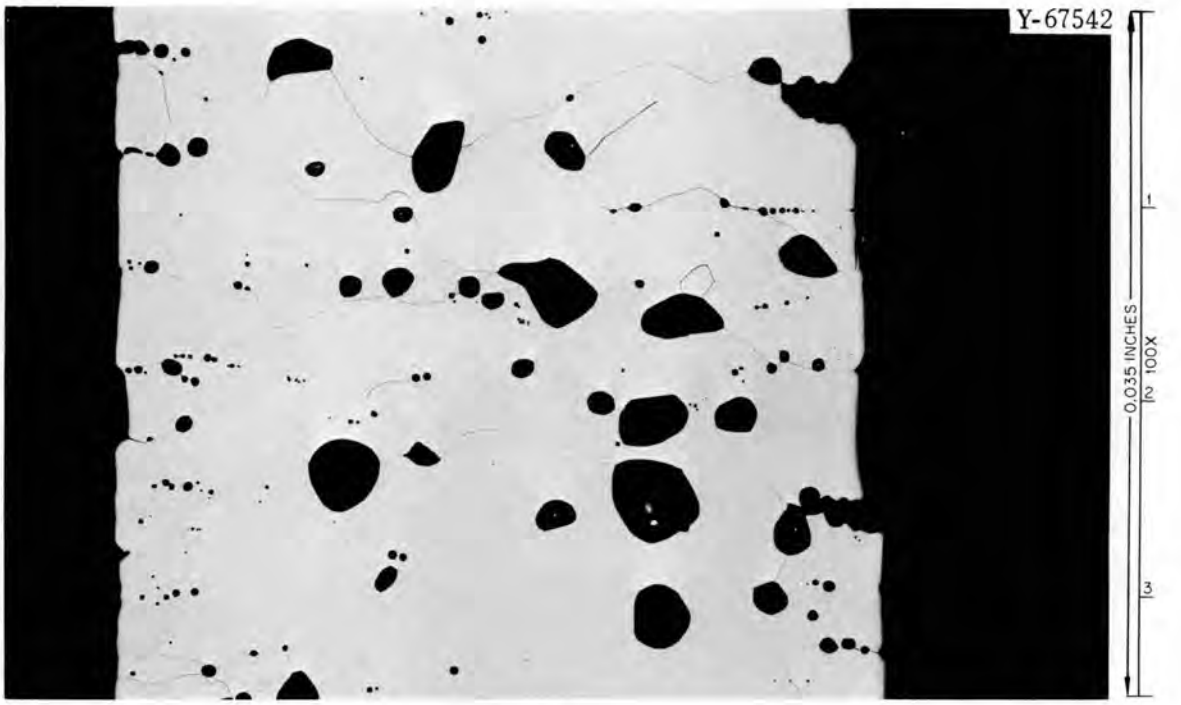

Fig. 23. Cross Section of TCD Tungsten from Lot PW-3, Tested at 2200°C and 2000 psi. Failed at 789.9 hr and 29.2% strain. Etchant: 50 parts NH_4OH and 50 parts H_2O_2.

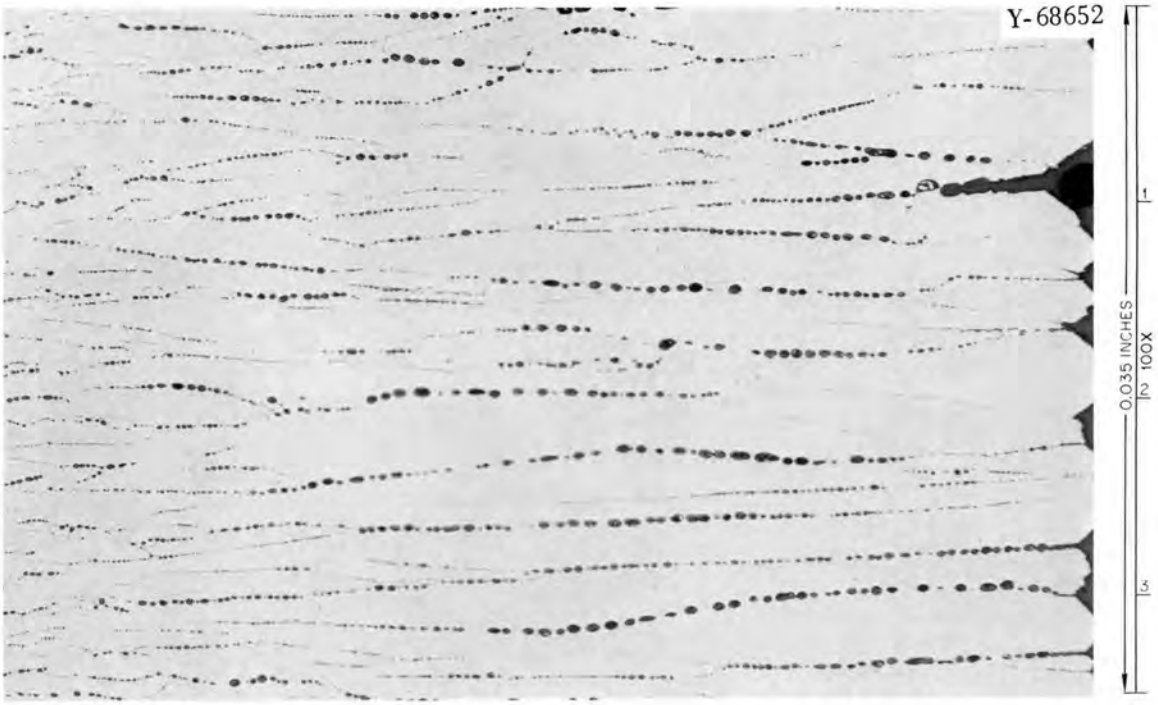

Fig. 24. Cross Section of a TCD Tungsten Specimen from Lot PW-19, Tested at 2200°C and 2000 psi. Failed at 4.3 hr and 4.2% strain. Etchant: 50 parts NH_4OH and 50 parts H_2O_2.

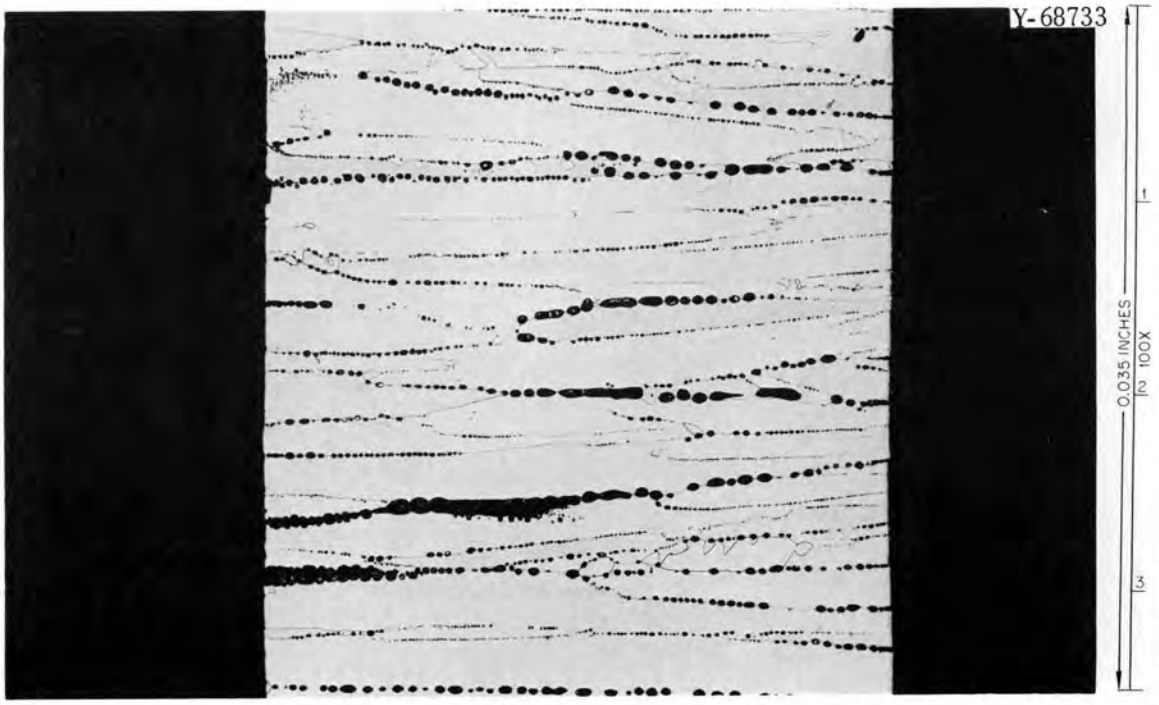

Fig. 25. Cross Section of TCD Tungsten from Lot PW-20, Tested at 2200°C and 2000 psi. Specimen failed at 1.86 hr and 15.6% strain. Etchant: 50 parts NH_4OH and 50 parts H_2O_2.

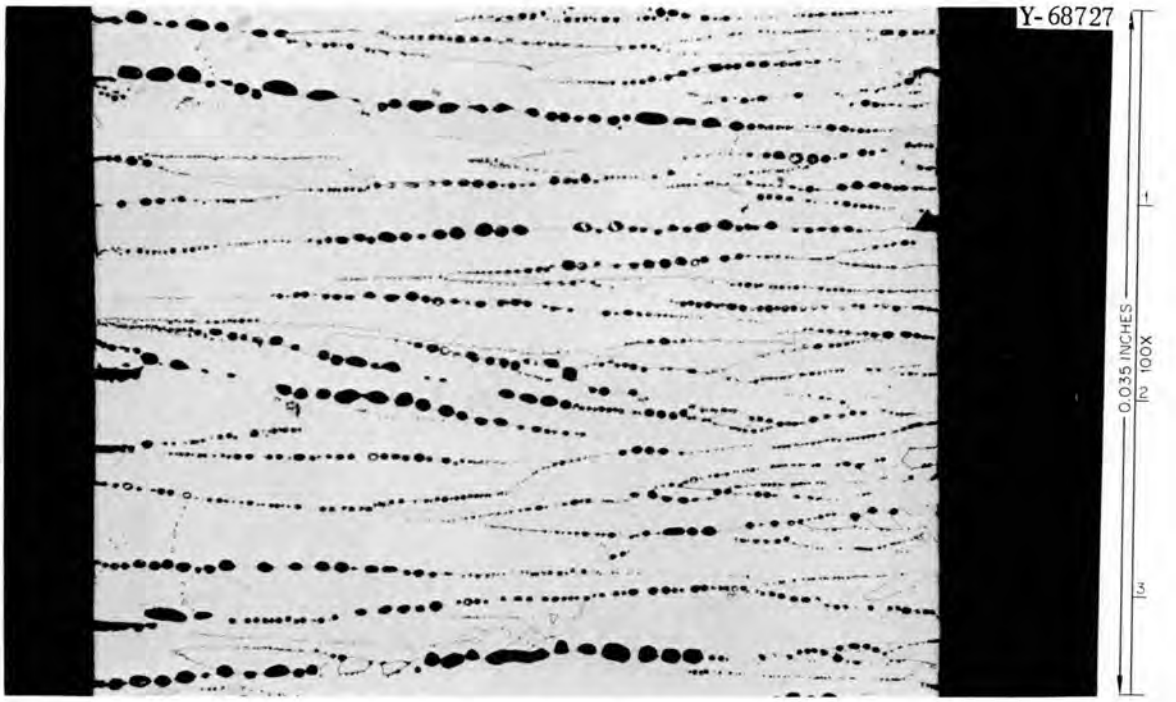

Fig. 26. Cross Section of a TCD Tungsten Specimen from Lot PW-23, Tested at 2200°C and 2000 psi. Failed after 5.05 hr and 21.8% strain. Etchant: 50 parts NH_4OH and 50 parts H_2O_2.

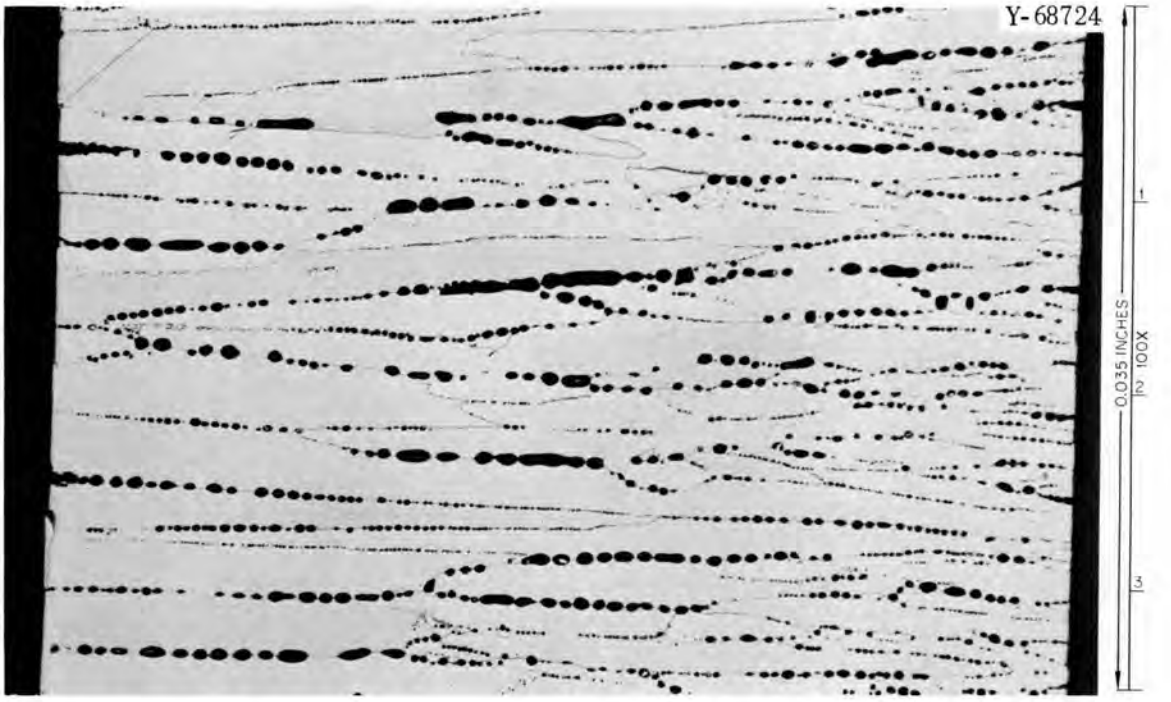

Fig. 27. Cross Section of a TCD Tungsten Specimen from Lot PW-24, Tested at 2200°C and 2000 psi. Failure occurred at 4.65 hr and 21.6% strain. Etchant: 50 parts NH_4OH and 50 parts H_2O_2.

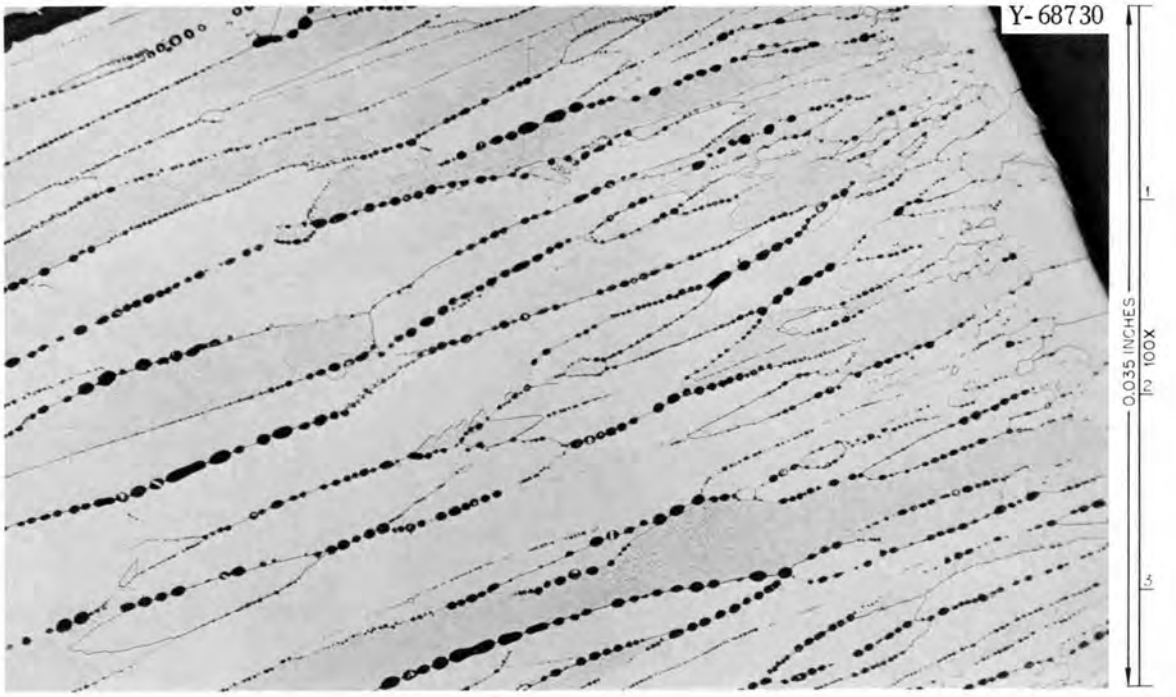

Fig. 28. Cross Section of a TCD Tungsten Specimen from Lot PW-23, Tested at 2200°C and 2000 psi. Annealed 90 hr at 1650°C prior to testing. Failure occurred at 5.3 hr and 21.9% strain. Etchant: 50 parts NH_4OH and 50 parts H_2O_2.

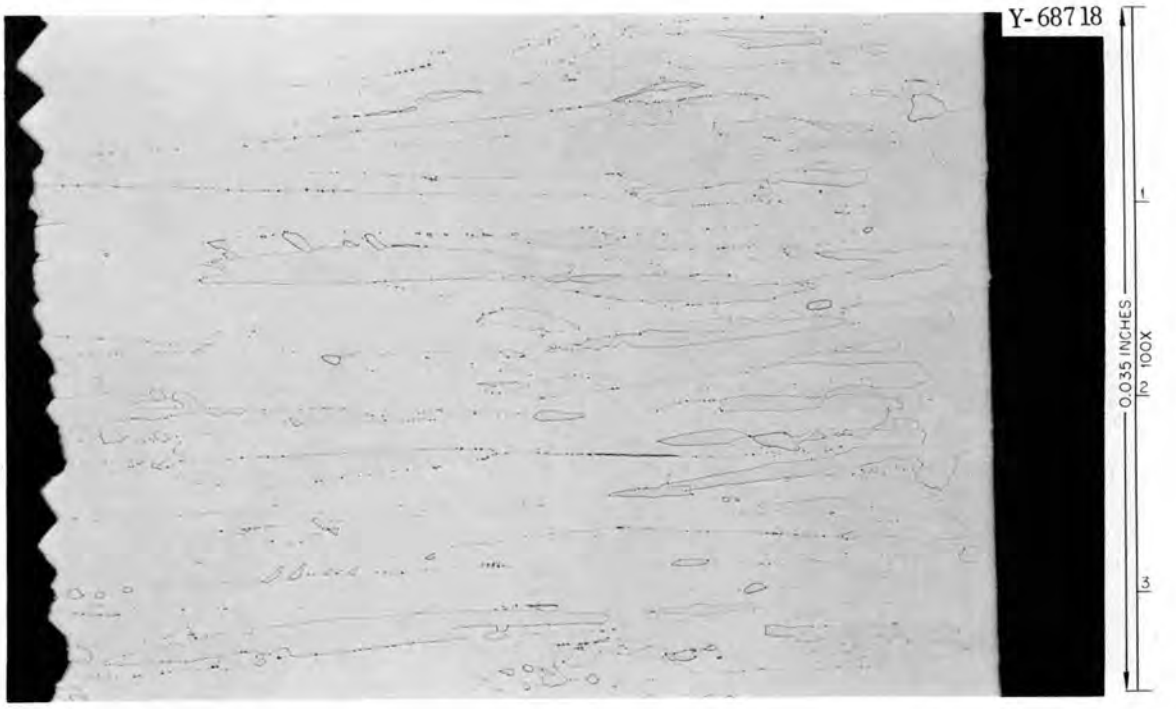

Fig. 29. Cross Section of a TCD Tungsten Specimen from Lot PW-19, annealed 5.3 hr and 2200°C. Etchant: 50 parts NH_4OH and 50 parts H_2O_2.

It is felt that the ductility of the TCD tungsten can be rationalized in terms of the microstructure. For extensive plastic deformation to occur at elevated temperatures, it is necessary that the grain boundaries be able to move. This requires that they move either by thermal activation (grain-boundary migration) or by shearing. Since shearing requires a shear stress across the grain boundaries, the predominance of perpendicular grain boundaries in the TCD microstructure will negate this mechanism. Hence, extensive plastic deformation would not be expected unless grain-boundary migration occurs. At 1650°C there was no change in the structure from the original columnar grains and all of the specimens, with only one exception, showed poor rupture ductility. At 2200°C there was a gradual transition to an equiaxial grain structure and an improvement in rupture ductility with increasing rupture life.

Although the ductility of this material can be rationalized in terms of the grain structure, it is felt that the extensive void formation cannot be ignored. In some of the specimens tested at 2200°C the void formation was so extensive that the two surfaces were likely connected by "void channels."

An explanation of the void formation must account for several experimental observations.

1. The concentration of the voids increased with increasing temperature.

2. Lot H-16 formed extensive voids at 1650°C, whereas the other lots formed only a few voids at this temperature.

3. A specimen was heated for 90 hr at 1650°C prior to heating to 2200°C and applying the stress. The void concentration was equal to that present in a specimen heated directly to 2200°C and stressed.

4. The voids formed very rapidly at 2200°C under stress and grew by coalescence during long tests. This suggests that an equilibrium void size is formed very rapidly under the stress. The coalescence of the voids with time is quite comparable to sintering in a powder-metallurgy product.

5. The voids reached a much larger size under stress than in the absence of a stress.

Creep conditions have been shown to produce voids in a large number of materials[13–16] and some argument exists concerning the role of impurities. However, the concentration of voids in the TCD tungsten at 2200°C is much higher than has been reported for other materials. The vacancy flux required to produce such large voids in so short a time would be unreasonably high.

All of the experimental observations seem consistent with the hypothesis that there is some impurity in the material that is insoluble in tungsten and has a reasonably high vapor pressure at elevated temperatures. As the material is heated, areas of high stress develop around the impurity and the tungsten deforms to relieve the pressure. Thus voids are nucleated and will grow as the tungsten deforms. Void coalescence and vacancy condensation are other mechanisms whereby the voids can grow. The role of an applied stress is to add to the stress already produced by the vapor pressure of the impurity and to cause even greater local deformation. It is quite likely that most of the responsible impurity will be released under stress since many of the voids extend to the surface.

Several attempts have been made to identify the responsible impurity(s). Void formation in this type of material is generally attributed to residual fluorine in some form. However, the possibility of some low-melting metallic impurity being responsible must also be considered. Analytical techniques that have sufficient reliability have not been developed to determine what metallic impurities are present in parts per million quantities. Hence, a positive identification of the responsible impurity has not been made at this time.

---

[13] R. W. Balluffi and L. L. Seigle, "Growth of Voids in Metals During Diffusion and Creep," Acta Met. 5, 449 (1957).

[14] N. Greenwood, D. R. Miller, and J. W. Suiter, "Intergranular Cavitation in Stressed Metals," Acta Met. 2, 250 (1954).

[15] E. S. Machlin, "Creep-Rupture by Vacancy Condensation," Trans. Met. Soc. AIME 206, 106 (1956).

[16] D. McLean, "A Note on the Metallography of Cracking During Creep," J. Inst. Metals 85, 468 (1956–57).

W–2% ThO_2 Alloy

The results of the creep tests run on the tungsten-base alloy W–2% ThO_2 are given in Table 4. The creep-rupture properties are shown in Figs. 30 and 31. The creep-rupture behavior at 1650°C is best described by a plot of linear stress vs logarithmic time – at 2200°C by a log-log plot of stress and time. The times to small strains are given in Table 4, but they exhibit a large amount of scatter. This is due mainly to slight changes in temperature that occurred near the start of the tests and gave the appearance of the specimen elongating. However, these results indicate the following trends. At 1650°C the time to 0.5% strain is about one-tenth that required to produce fracture, the time to 2% strain is one-fourth that to fracture. At 2200°C the spread between the time to reach 0.5% strain and the time to fracture decreases with increasing rupture life (or decreasing stress). A test which failed in 1 hr would reach 0.5% strain in 0.01 hr. A test which fails in 150 hr would read 0.5% strain in 90 hr. The behavior at 2200°C is particularly attractive from a design standpoint. The material would deform only slightly at low stresses, but would be able to strain to relieve high stresses due to any transients.

Figures 32 and 33 show plots of the minimum creep rate and the time to rupture. Again the 1650°C data are linear on a semilog plot and the 2200°C data are linear on log-log coordinates.

The 1-hr anneal at 2200°C prior to testing at 1650°C reduced the strength over that of the as-received material. This reduction in strength is probably due to recrystallization. The recrystallization temperature for 80% cold-worked W–2% ThO_2 is reported[14] to be 2195°C (1-hr anneal). The amount of cold work in the as-received material is not known, but metallographic examination showed that recrystallization did occur at 2200°C.

Figure 34 shows the elongation at rupture vs the rupture life. At 1650°C the ductility reached a constant value of about 9% for rupture

---

[14]H. G. Sell et al., "Physical Metallurgy of Tungsten and Tungsten-Base Alloys," WADD TR 60-37, Part II (May 1961).

Table 4. Creep-Rupture Properties of W–2% ThO_2

Test Number	Stress (psi)	Time to Indicated Strain, hr					Reduction in Area (%)	Minimum Creep Rate (%/hr)
		0.5%	1%	2%	Rupture	Elongation Rupture (%)		
				Tested at 1650°C				
5085	25,000	0.10	0.2	0.41	0.8	21.9	74.8	5.0
5168	20,000				2.65	15.6	43.0	1.8
5188	17,500	0.30	0.8	3.4	10.65	11.0	46.3	0.365
5095	15,000	0.35	1.0	3.6	25.75	9.4	21.6	0.23
5097	10,000	1	7	20	112.3	9.4	5.5	0.053
4070	8,000				237.9	9.4	5.1	0.039
5170	6,000	15	53	140	437.7	9.4	2.6	0.0078
5169[a]	10,000	0.05	0.10	0.23	4.35	21.9	20.5	2.66
5167[a]	6,000	1.7	5.5	16.3	45.5	9.4	4.8	0.10
5181[a]	4,500	1	2	10	121.7	6.25	1.6	0.020
				Tested at 2200°C				
5084	5,000	0.012	0.023	0.05	0.55	9.4	7.9	10.3
5121	2,500	0.1	0.3	1.6	11.65	4.8	1.6	0.20
5180	1,750	11	26	50	70.4	6.25	2.4	0.034
5214	1,400	88	123	152	157.1	9.4	2.4	0.0048

[a]Annealed 1 hr at 2200°C prior to testing.

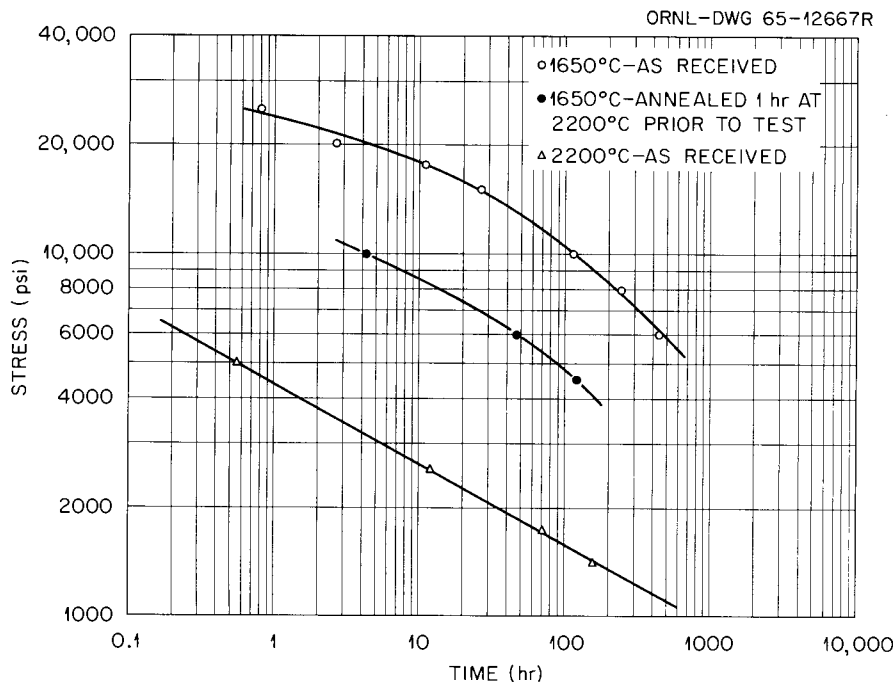

Fig. 30. Creep-Rupture Properties of W–2% ThO_2.

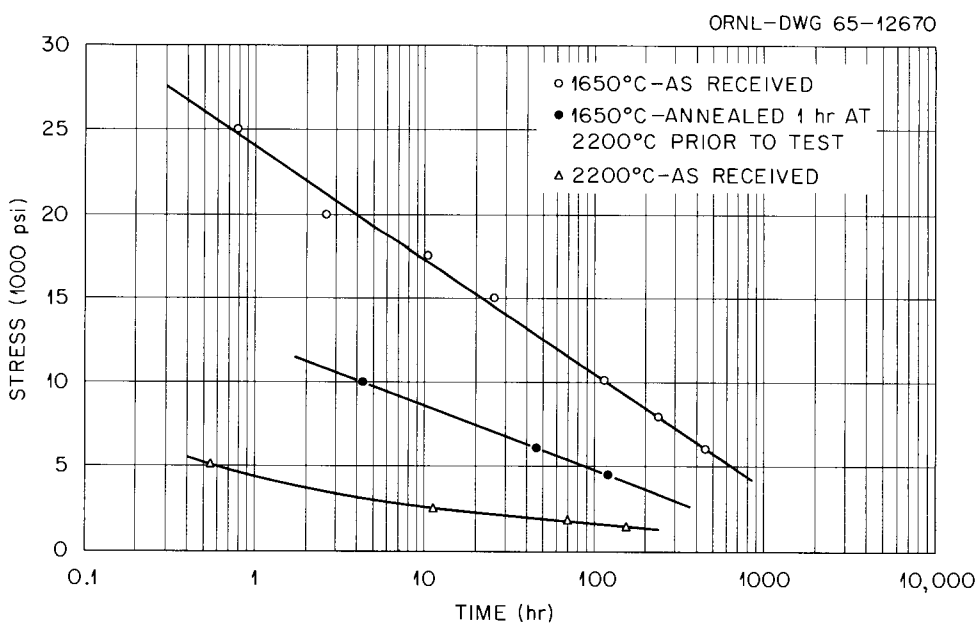

Fig. 31. Creep-Rupture Properties of W–2% ThO_2.

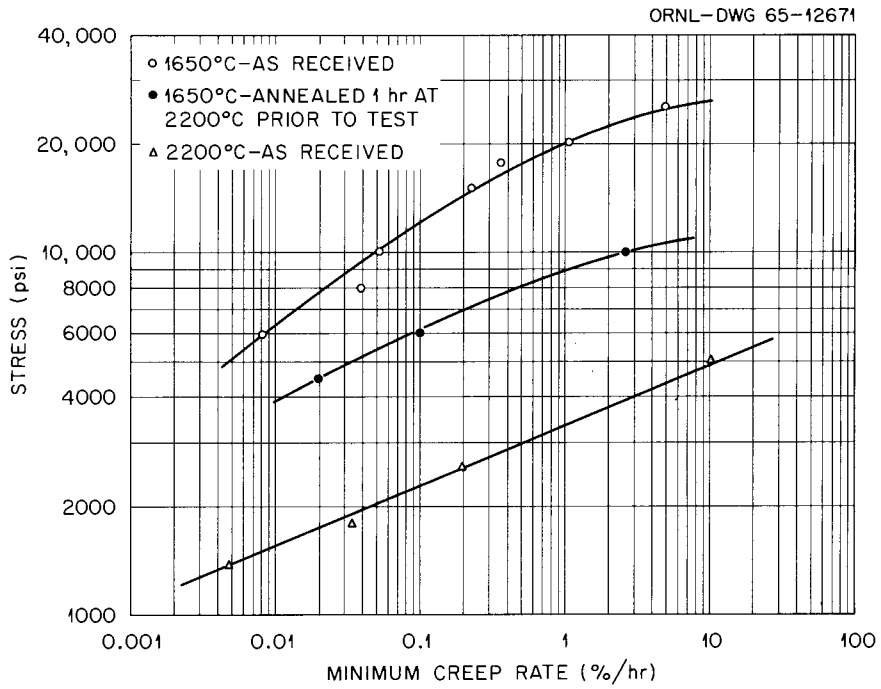

Fig. 32. Minimum Creep Rate of W–2% ThO_2.

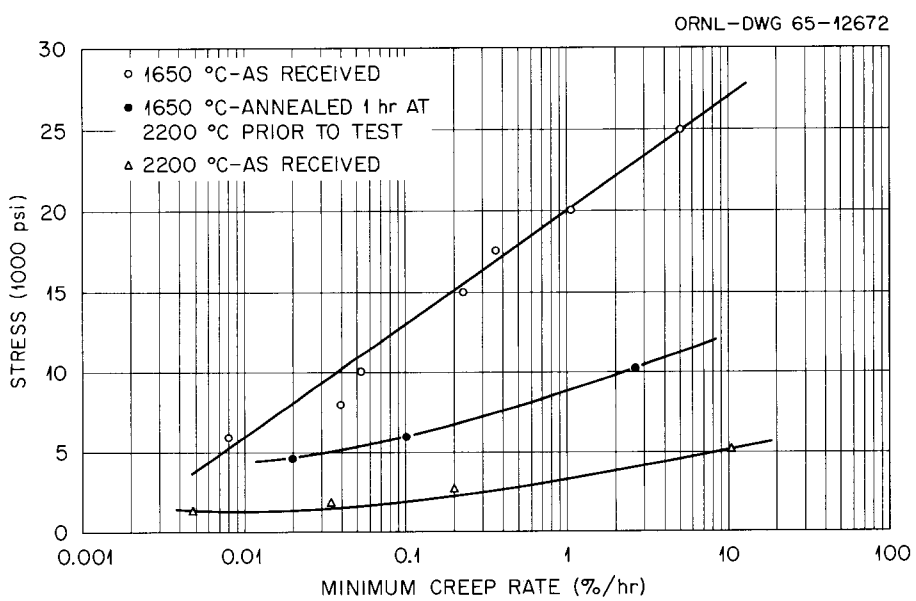

Fig. 33. Minimum Creep Rate of W–2% ThO_2.

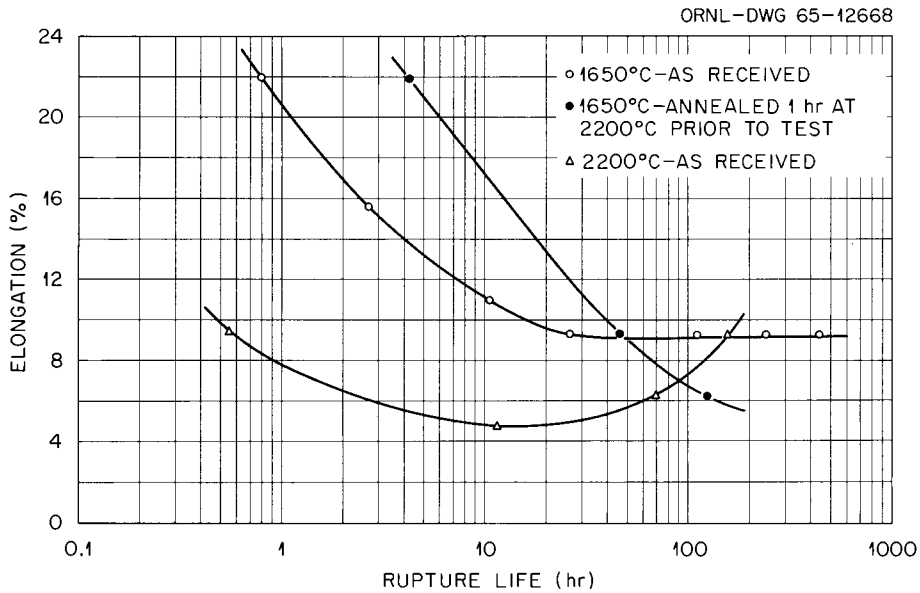

Fig. 34. Elongation at Rupture vs the Rupture Life of W–2% ThO_2.

lives of over 20 hr. The material annealed 1 hr at 2200°C and tested at 1650°C exhibited the same behavior except that the ductility was higher at rupture times less than 50 hr and less for longer rupture times. At 2200°C the rupture elongation decreased with increasing rupture time up to about 10 hr where it increased with increasing rupture time. Hence, it appears that ductilities in the range of 6 to 10% can be expected for rupture lives over 100 hr at both test temperatures. The reduction in area data (Fig. 35) shows similar trends with the exception that they do not seem to level off at times in excess of 10 hr for the 1650°C data. However, the reduction-in-area values are quite low for rupture times in excess of 100 hr with values of 2 to 5% being common to both temperatures.

Figure 36 shows the minimum creep rate-rupture life correlation for W–2% ThO_2. Although the correlation is reasonably good, the data seem to be on three different lines – one for each test condition. The lines have slopes of 1.0, 0.72, and 0.85 for the material as-received and tested at 1650°C, annealed at 2200°C and tested at 1650°C, and as-received and tested at 2200°C, respectively.

Several of the specimens were examined metallographically. Figure 37 shows the microstructure of the as-received material. The material appears to be quite heavily cold worked. Figure 38 shows the

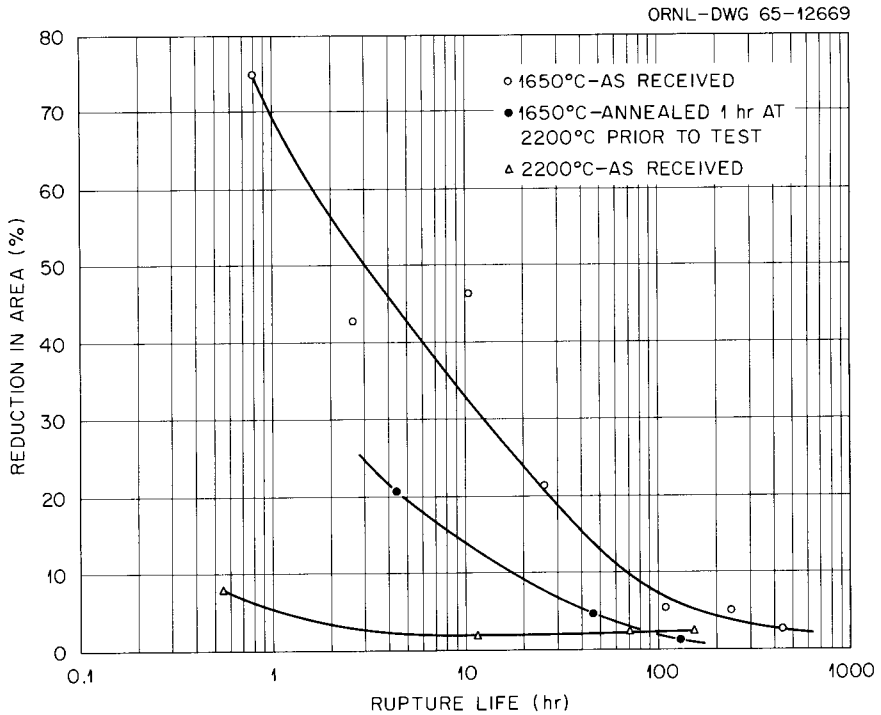

Fig. 35. Reduction in Area of W–2% ThO_2.

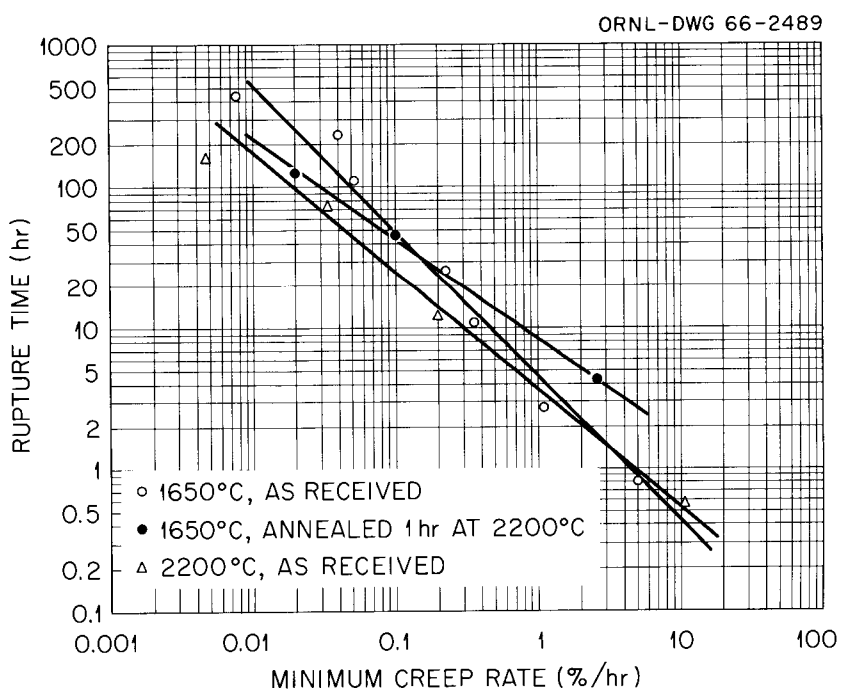

Fig. 36. The Minimum Creep Rate-Rupture Life Correlation for W–2% ThO_2.

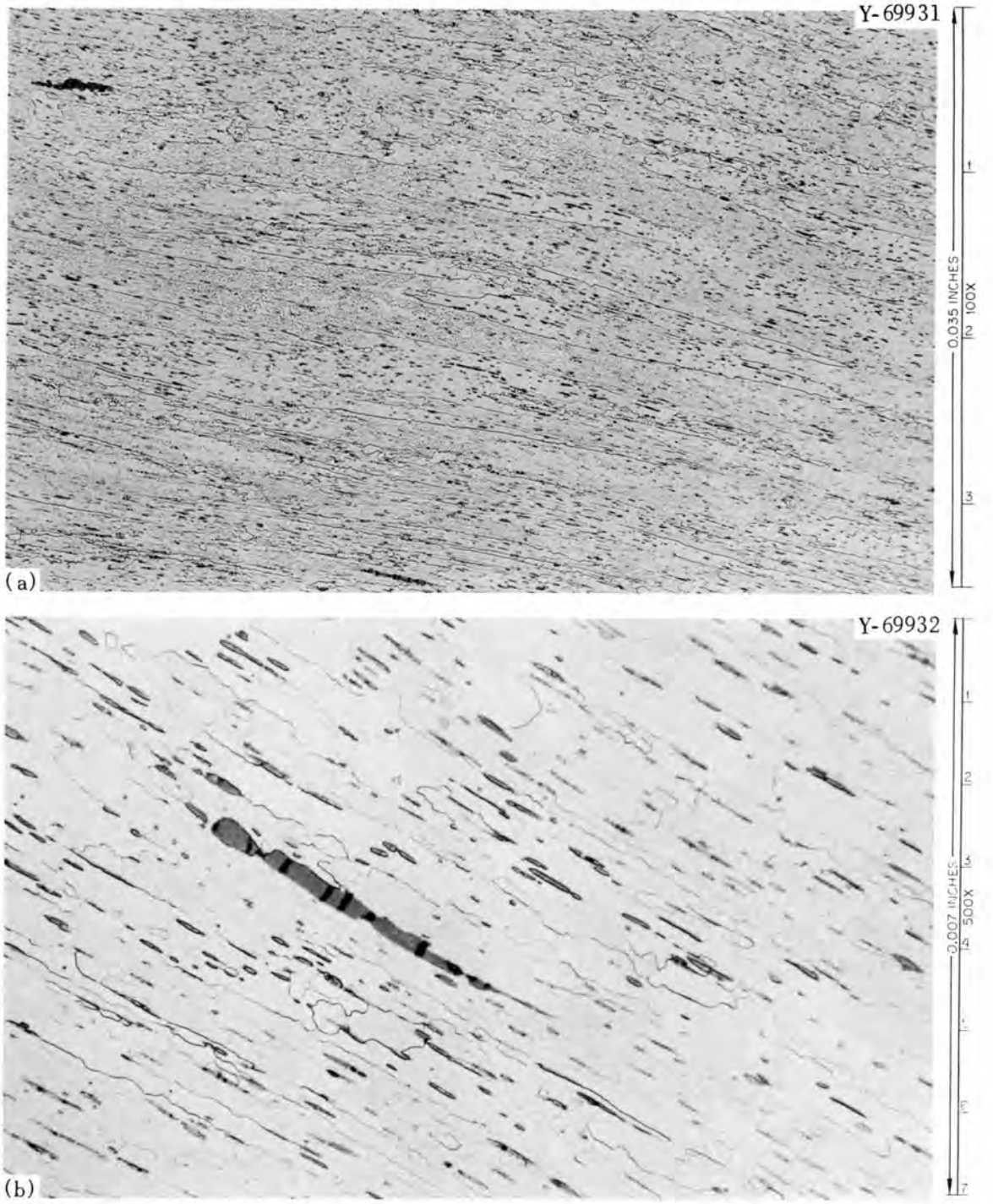

Fig. 37. Photomicrographs of W–2% ThO_2 in the As-Received Condition. Etchant: 50 parts NH_4OH and 50 parts H_2O_2.

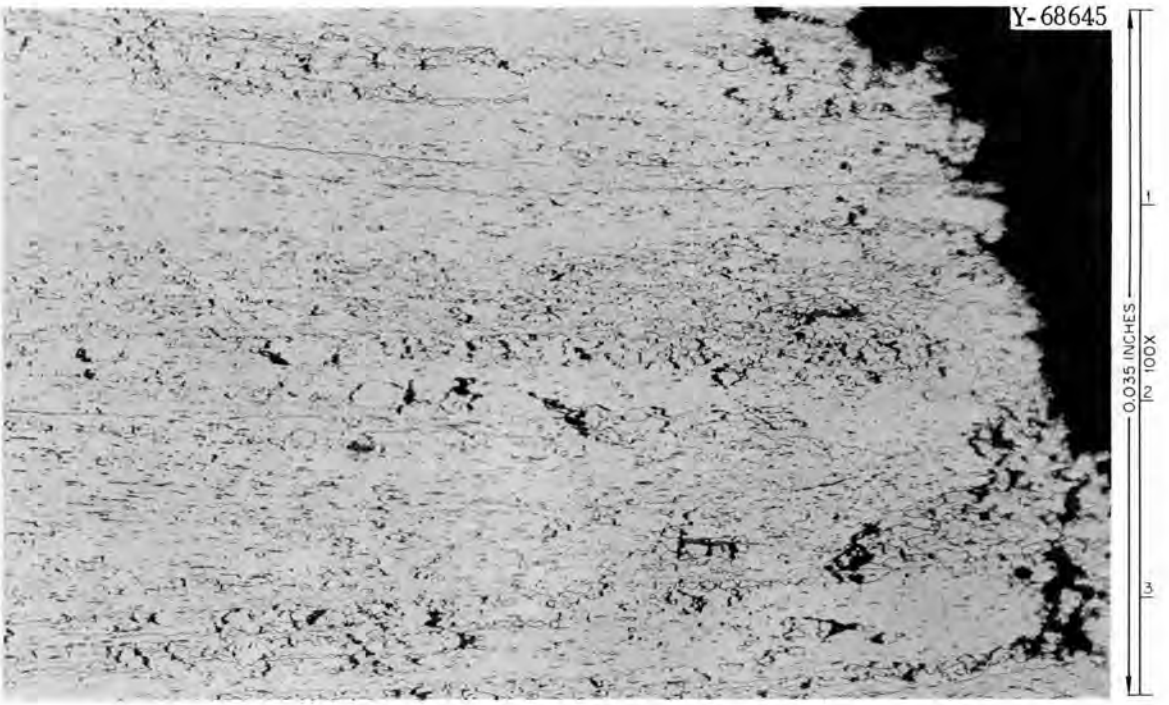

Fig. 38. Photomicrograph of a W–2% ThO_2 Specimen Tested at 1650°C and 15,000 psi. Failure occurred in 25.75 hr with 9.4% strain. Etchant: 50 parts NH_4OH and 50 parts H_2O_2.

microstructure of a specimen tested at 1650°C and 15,000 psi. Failure occurred in 25.75 hr with 9.4 strain. The fracture is primarily transgranular although there are numerous intergranular cracks. The microstructure of a specimen tested at 1650°C and 6000 psi is shown in Fig. 39. This specimen failed in 437.7 hr with 9.4% strain. Numerous intergranular cracks have formed and the fracture appears to be predominately intergranular. Figure 40 shows the microstructure of a specimen annealed 1 hr at 2200°C and tested at 1650°C. The specimen failed in 4.35 hr with 21.9% strain. The 2200°C anneal caused complete recrystallization. Extensive grain-boundary cracking occurred and the fracture was predominately intergranular. Figure 41 shows an as-received specimen tested at 2200°C and 5000 psi. Failure occurred at 0.55 hr with 9.4% strain. The grain size formed under stress at 2200°C is smaller than that formed in a 1-hr anneal without stress (Fig. 40). Numerous intergranular cracks have formed and the failure is intergranular. The test specimens tested at 2200°C for periods of 70.4 and

Fig. 39. Photomicrograph of a W–2% ThO_2 Specimen Tested at 1650°C and 6000 psi. Failure occurred in 437.7 hr with 9.4% strain. Etchant: 50 parts NH_4OH and 50 parts H_2O_2.

157.1 hr were examined metallographically and found to be similar to the specimen shown in Fig. 41. Hence, the ThO_2 dispersion seems very effective in preventing the grain growth at 2200°C which occurred in the powder-metallurgy tungsten (Fig. 12).

Sylvania A

The results of creep tests on Sylvania A are summarized in Table 5. The tests on this material exhibit considerable scatter. This is felt to be due to flaws in the material since there were several obvious surface defects. The creep-rupture results at 2200 and 1650°C are shown in Fig. 42. The rupture ductility is shown as a function of rupture life in Fig. 43. The ductility at 1650 and 2200°C is about 5% up to a

Fig. 40. Photomicrograph of a W–2% ThO_2 Specimen Annealed 1 hr at 2200°C and Tested at 10,000 psi and 1650°C. Failure occurred after 4.35 hr with 21.9% strain. Etchant: 50 parts NH_4OH and 50 parts H_2O_2.

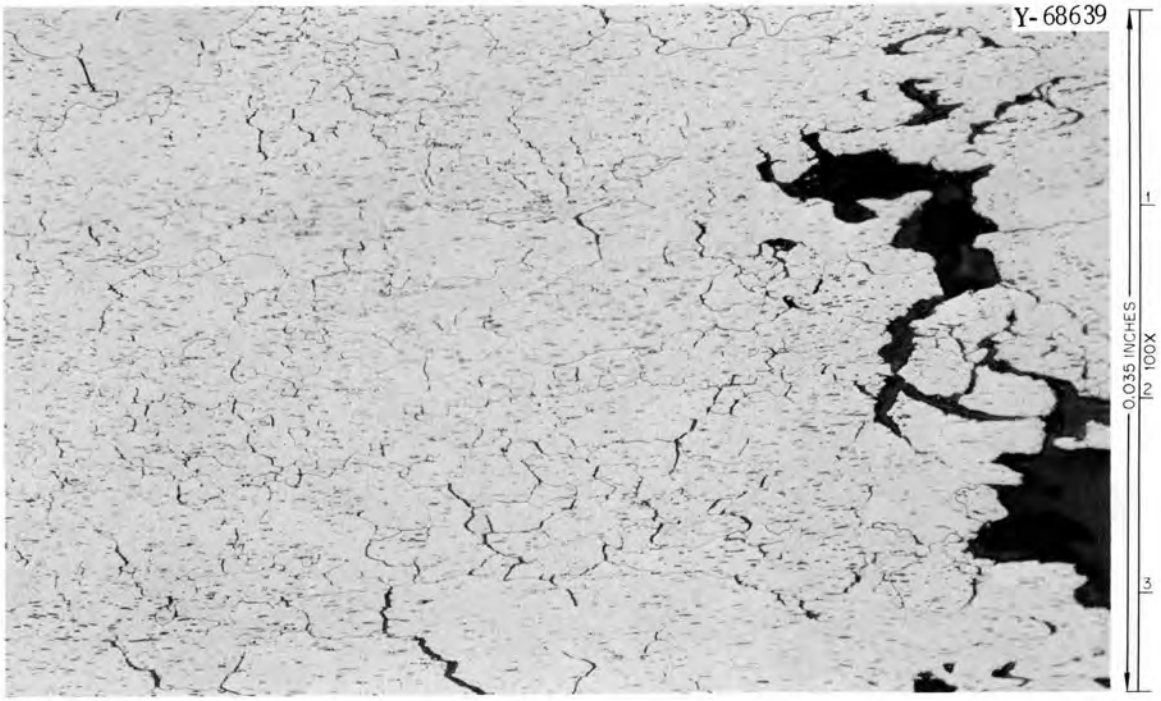

Fig. 41. Photomicrograph of a W–2% ThO_2 Specimen Tested at 2200°C and 5000 psi. Failure occurred after 0.55 hr with 9.4% strain. Etchant: 50 parts NH_4OH and 50 parts H_2O_2.

Table 5. Creep-Rupture Properties of Sylvania A

Test Number	Stress (psi)	Time to Indicated Strain, hr				Rupture Elongation (%)	Minimum Creep Rate (%/hr)
		1%	2%	5%	Rupture		
			Tested at 1650°C				
3705	10,000	1.2	4.3	15	15.2	6.2	0.26
5296[a]	8,000	1.0	2.0	11	194.4	29.7	0.096
3836	6,000	5	30	170	511.1	12.3	0.018
			Tested at 2200°C				
4069	6,000				0.1	~0	
3678	4,000	0.20	0.47	0.63	0.68	6.25	0.23
3679	2,000	2.7	4.3	7.4	7.75	6.40	0.38
3688	1,000	7.0	16	39	46.7	7.3	0.11
5096[a]	1,000	3.0	8	24	68.5	14.9	0.17
5098	600	5.0	10	30	643.8	80.2	0.065

[a]Both surfaces lapped.

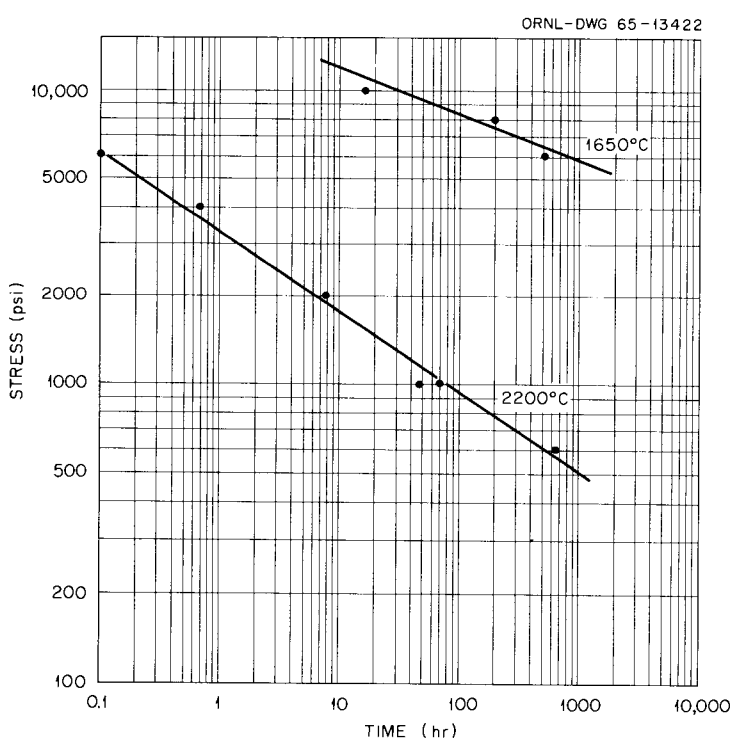

Fig. 42. Creep-Rupture Properties of Sylvania A.

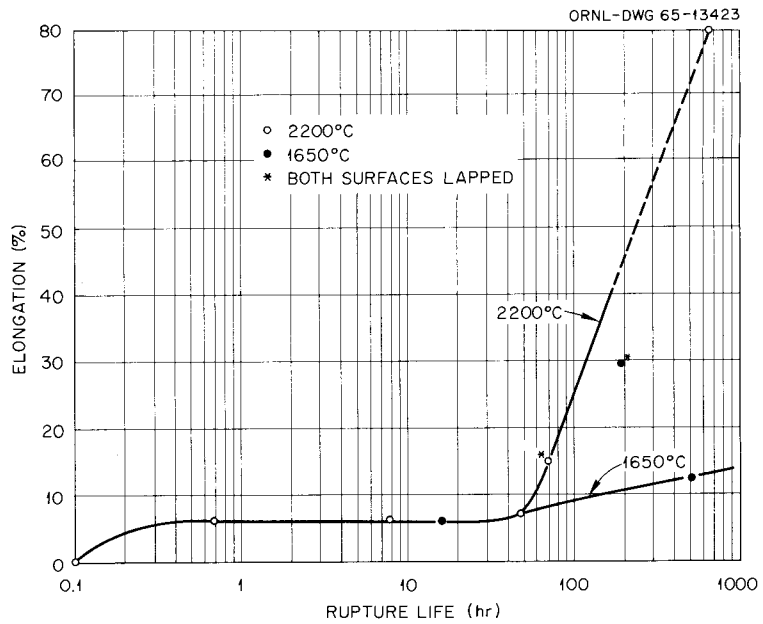

Fig. 43. Fracture Ductility of Sylvania A.

rupture life of 50 hr. Tests of longer duration indicate an increase in the ductility. The high rupture ductility of the specimen at 2200°C with a rupture life of 644 hr is questionable because of the unusual metallographic appearance of the specimen. Very extensive cracking and void formation occurred throughout the specimen. However, chemical analysis showed that the specimen did contain hafnium, so a mixup of test material is doubtful. Some of the specimens were surface lapped prior to testing, but this did not have a significant effect.

Figure 44 shows the microstructure of the as-received material. The material was characterized by a heavily cold-worked structure and patches of precipitate which are probably HfC. The microstructure typical of a specimen tested at 1650°C is shown in Fig. 45. This specimen was tested at 6000 psi and failed after 511.1 hr with 12.3% elongation. The material has partially recrystallized. Numerous intergranular cracks have formed but the fracture appears to be both intergranular and transgranular. Figure 46 shows the microstructure typical of a specimen tested at 2200°C. This specimen was tested at 1000 psi and failed after 46.7 hr with 7.3% strain. The structure is completely recrystallized, but there is no evidence of extensive grain growth. Intergranular cracking is extensive and the fracture is intergranular.

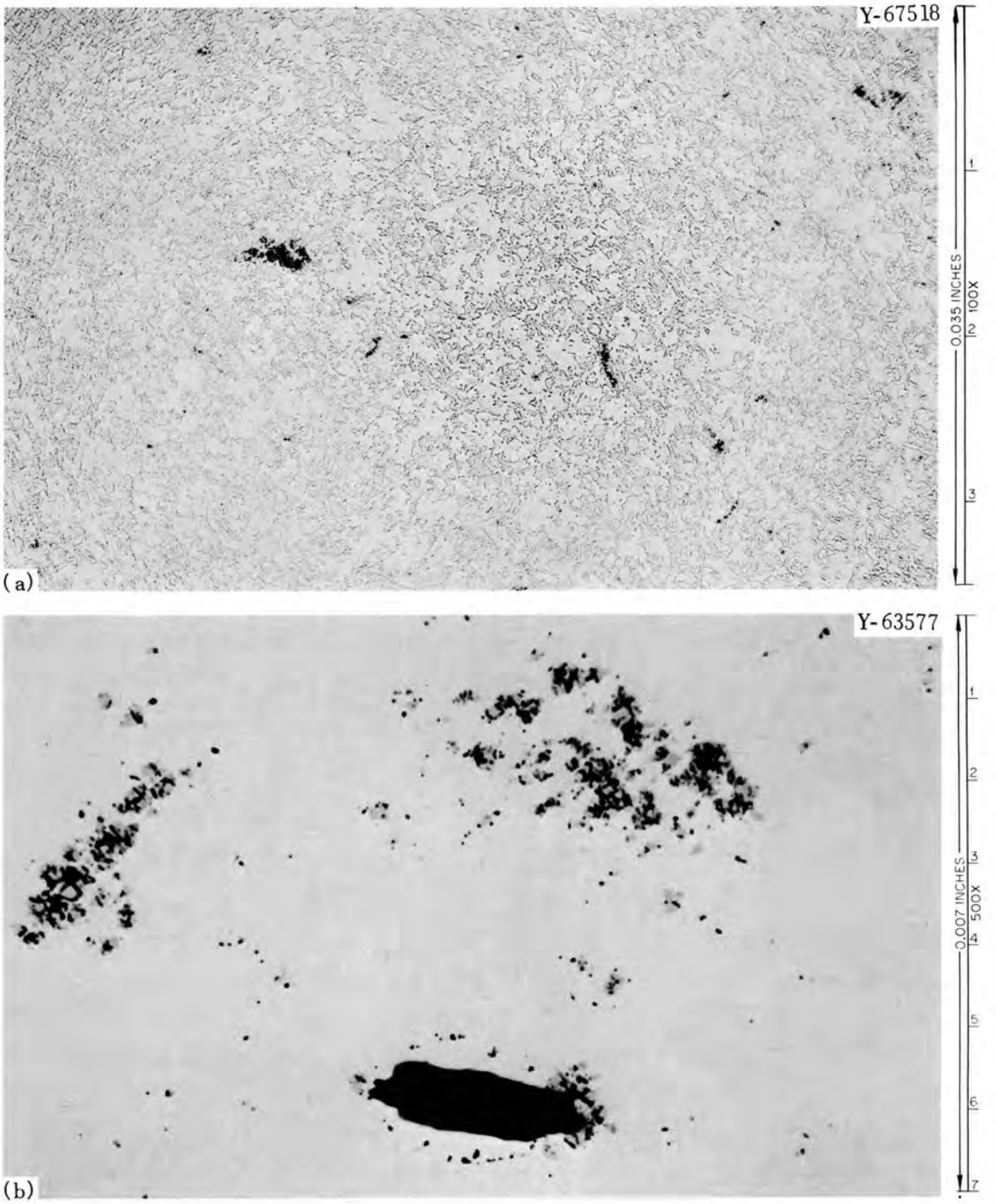

Fig. 44. Photomicrographs of a Sylvania A Specimen in the As-Received Condition. View in plane of sheet. (a) Etchant: 50 parts NH_4OH and 50 parts H_2O_2. (b) As polished.

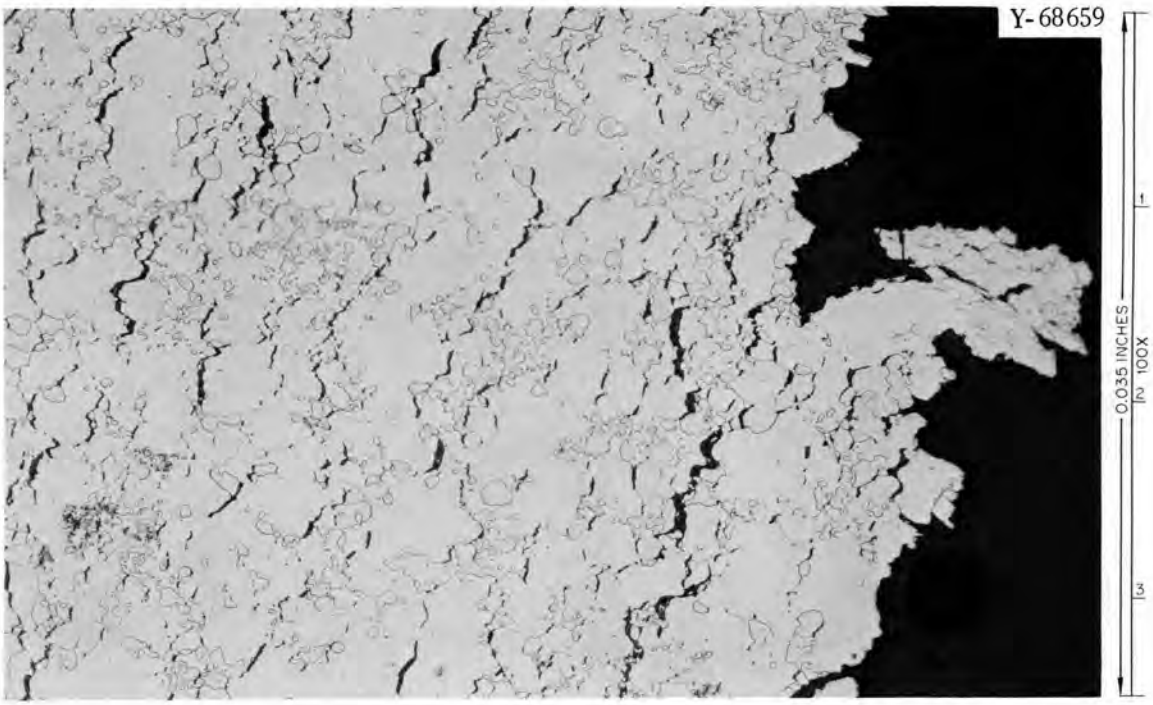

Fig. 45. Photomicrograph of a Sylvania A Specimen Tested at 1650°C and 6000 psi. Failure occurred after 511.1 hr with 12.3% strain. Etchant: 50 parts NH_4OH and 50 parts H_2O_2.

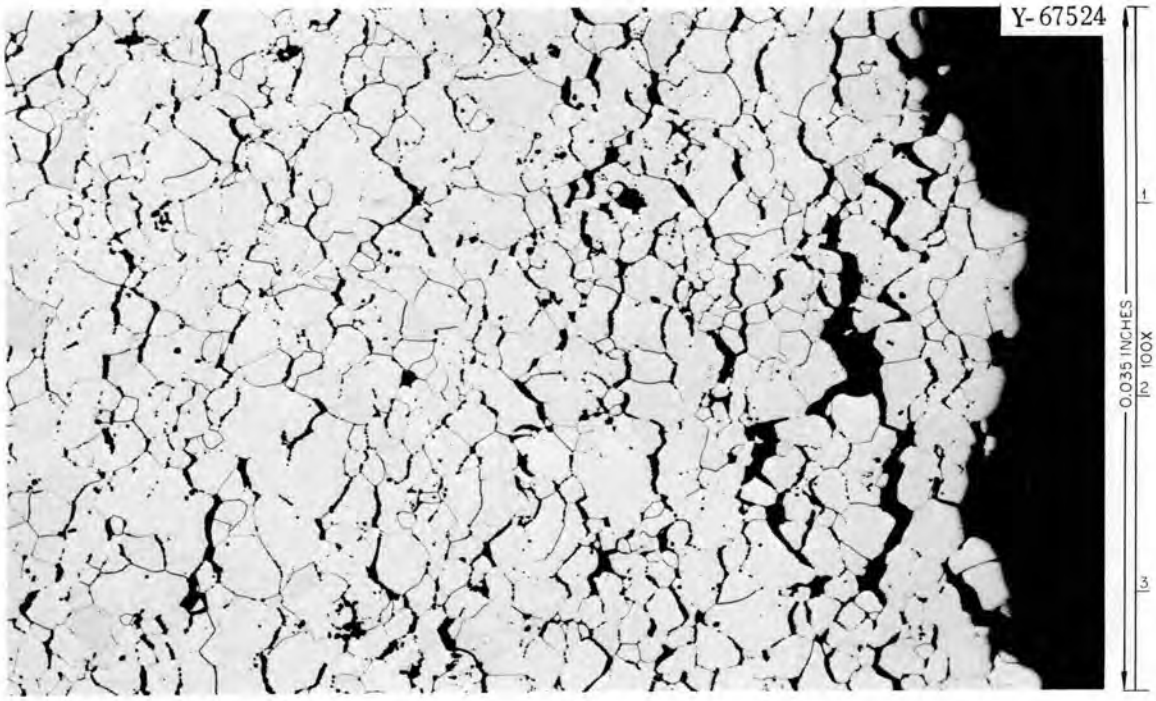

Fig. 46. Photomicrograph of a Sylvania A Specimen Tested at 2200°C and 1000 psi. Failure occurred after 46.7 hr with 7.3% strain. Etchant: 50 parts NH_4OH and 50 parts H_2O_2.

SUMMARY AND CONCLUSIONS

In this study creep-rupture properties have been obtained at 1650 and 2200°C for powder-metallurgy tungsten, several heats of TCD tungsten, W–2% thoria, and Sylvania A (W–0.5% Hf–0.2% C). The comparative creep-rupture properties are shown in Fig. 47. At 1650°C W–2% ThO_2 is the strongest up to rupture lives of above 500 hr where Sylvania A seems to offer the best strength. The powder-metallurgy and TCD tungsten are the weakest. Although there are distinct differences between the alloys in strength, it is interesting that the stress to produce rupture in a given time never varies by more than a factor of 2 at 1650°C. At 2200°C the order of strengths from greatest to least is W–2% ThO_2, powder-metallurgy and TCD tungsten, and Sylvania A. The addition of 0.05 wt % Hf (mp = 2200°C) to tungsten (mp = 3410°C) seems to reduce the strength of the latter. About half of the hafnium should be present as HfC and the rest would be present in solution in the tungsten. A reduction in the hafnium content might improve the high-temperature creep strength of the alloy. Again the spread in strengths is within a factor of 2 for all four materials.

The comparative elongations of the test materials are in Table 6. At 1650°C the ductility of the powder-metallurgy tungsten is high, that of TCD tungsten low, and that of Sylvania A and W–2% ThO_2 moderate. At 2200°C all materials show good ductility, except W–2% ThO_2 whose ductility is moderate.

All materials exhibited better grain size stability at 2200°C than the powder-metallurgy tungsten. The TCD tungsten had a columnar grain structure which was quite stable. However, this material formed voids at 2200°C which were noted to grow under an applied stress. These voids are thought to be associated with impurities in the material.

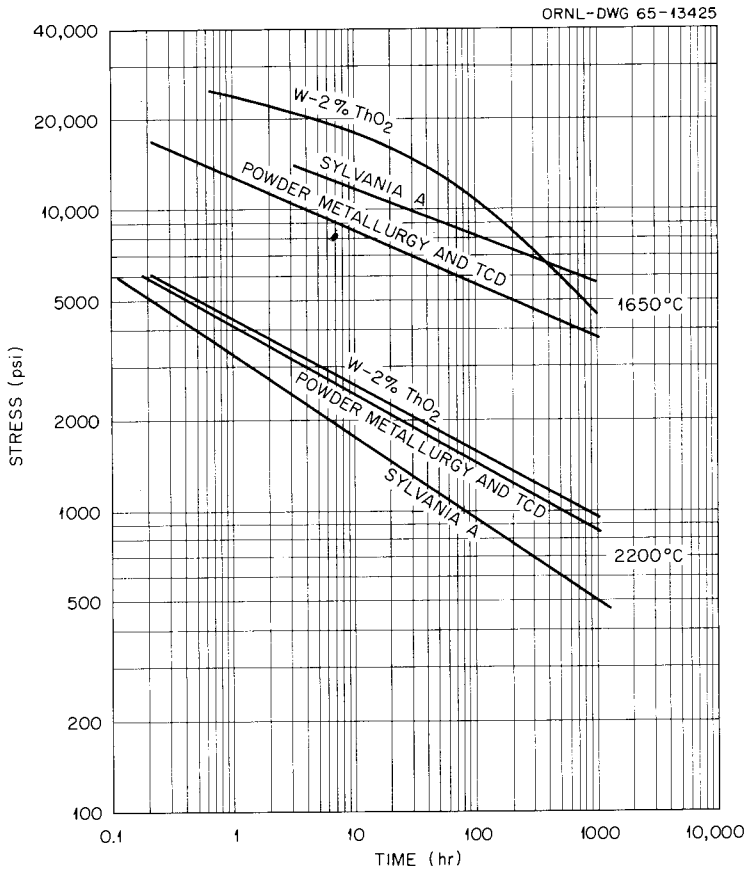

Fig. 47. Comparative Creep-Rupture Properties of Several Tungsten-Base Alloys.

Table 6. Comparative Elongations of Several Tungsten-Base Alloys

Material	Elongation at 100 hr Rupture Life, %	
	1650°C	2200°C
Powder Metallurgy	32	12–19
TCD	3–5	17–35
Sylvania A	9	20–25
W–2% ThO_2	9	8

ACKNOWLEDGEMENT

The author gratefully acknowleges the assistance of E. B. Bolling who performed the experimental work and H. R. Tinch who did the metallographic work. The services of the Analytical Chemistry Division who performed the various chemical analyses and the Graphic Arts Department who prepared the graphical illustrations were very helpful. The manuscript was prepared by the Metals and Ceramics Reports Office. The author is grateful to J. R. Weir, R. L. Stephenson, A. C. Schaffhauser, and D. A. Douglas for reviewing this report.

ORNL-3992
UC-25 — Metals, Ceramics, and Materials

INTERNAL DISTRIBUTION

1–3. Central Research Library
4–5. ORNL — Y-12 Technical Library
Document Reference Section
6–25. Laboratory Records
26. Laboratory Records, ORNL R.C.
27. ORNL Patent Office
28. R. J. Arsenault
29. John Askill
30. R. J. Beaver
31. H. Beutler
32. E. E. Bloom
33. G. E. Boyd
34. W. H. Cook
35. G. L. Copeland
36. C. W. Cunningham
37. J. E. Cunningham
38. W. W. Davis
39. J. H. DeVan
40. J. R. DiStefano
41. W. S. Ernst, Jr.
42. S. T. Ewing
43. J. I. Federer
44. J. H Frye
45. W. Fulkerson
46. Karl W. Haff
47. R. Heestand
48–52. M. R. Hill
53. T. S. Kress
54. C. E. Larson
55. C. F. Leitten, Jr.
56. A. P. Litman
57. B. Loh
58. H. G. MacPherson
59–63. H. E. McCoy
64. C. J. McHargue
65. W. R. Martin
66. F. H. Patterson
67. L. R. Phillips (Y-12)
68. W. C. Robinson
69. A. C. Schaffhauser
70. C. E. Sessions
71. J. L. Scott
72. M. J. Skinner
73. G. M. Slaughter
74. R. L. Stephenson
75. J. O. Stiegler
76. J. T. Venard
77. C. S. Yust
78. A. M. Weinberg
79. J. R. Weir
80. J. W. Woods
81. G. T. Yahr
82. A. F. Zulliger
83. M. B. Bever (Consultant)
84. A. R. Kaufmann (Consultant)
85. J. A. Krumhansl (Consultant)
86. T. A. Read (Consultant)

EXTERNAL DISTRIBUTION

87. G. M. Anderson, AEC, Washington
88. C. H. Armbruster, Wright-Patterson AFB
89–91. V. P. Calkins, General Electric, NMPO
92. S. S. Christopher, Combustion Engineering, Inc.
93–95. D. F. Cope, AEC, Oak Ridge Operations Office
96. J.W.R. Creagh, NASA, Lewis Research Center
97. J. Davis, Jet Propulsion Laboratory
98. R. W. Dayton, Battelle Memorial Institute
99. G. K. Dicker, AEC, Washington
100. E. M. Douthett, AEC, Washington

101. J. K. Elbaum, Code MAMP, Wright-Patterson AFB
102. D. DeHalas, Pacific Northwest Laboratory, Richland
103. D. C. Goldberg, Westinghouse Astronuclear Laboratory
104–105. D. H. Gurinsky, Brookhaven National Laboratory
106. R. Hall, NASA, Lewis Research Center
107. R. C. Hamilton, Institute for Defense Analyses, 1666 Connecticut Avenue, N.W., Washington, D.C.
108. E. E. Hoffman, General Electric, Cincinnati
109. W. R. Holman, Lawrence Radiation Laboratory
110. C. Johnson, Space Nuclear Systems Division, Space Electric Power Office, AEC, Washington 20545
111. J. S. Kane, University of California
112. J. J. Lombardo, NASA, Lewis Research Center
113. J. J. Lynch, NASA, Washington
114. T. P. Moffitt, NASA, Lewis Research Center
115–117. T. A. Moss, NASA, Lewis Research Center
118. R. A. Noland, Argonne National Laboratory
119. Louis Rosenblum, NASA, Lewis Research Center
120. A. J. Rothman, Lawrence Radiation Laboratory
121. N. D. Sanders, NASA, Lewis Research Center
122. H. Schwartz, NASA, Lewis Research Center
123. F. C. Schwenk, AEC, Washington
124–128. J. M. Simmons, AEC, Washington
129. D. K. Stevens, AEC, Washington
130. J. A. Swartout, Union Carbide Corporation, New York
131. G. W. Wensch, AEC, Washington
132. M. J. Whitman, AEC, Washington
133. Division of Research and Development, AEC, ORO
134–454. Given distribution as shown in TID-4500 under Metals, Ceramics, and Materials category (75 copies – CFSTI)

General Electric Thermionic

$^{244}Cm_2O_3$ – 1 kw_t – 1650°C

Stress rate safety factor	Allowable pressure rate, psi/hr	Capsule dimensions, in. i.d.	o.d.	length	Capsule wt, lb
Length/diameter = 3					
2	0.030	2.25	2.580	7.74	6.9
2	0.045	2.00	2.462	7.38	8.4
2	0.055	1.875	2.420	7.26	9.4
2	0.065	1.750	2.372	7.12	10.0
2	0.080	1.625	2.378	7.14	11.6
2	0.100	1.500	2.450	7.35	14.7
2	0.120	1.375	2.536	7.61	18.1
2	0.145	1.250	2.758	8.27	25.8
3	0.030	2.25	2.776	8.33	12.2
3	0.050	1.875	2.686	8.06	16.2
3	0.060	1.750	2.718	8.15	18.9
3	0.070	1.625	2.752	8.25	21.6
3	0.085	1.500	2.936	8.81	29.3
3	0.100	1.375	3.208	9.62	41.6
4	0.030	2.25	2.976	8.93	18.6
4	0.040	2.00	2.928	8.78	21.7
4	0.045	1.875	2.896	8.69	22.7
4	0.055	1.750	3.032	9.09	29.5
4	0.070	1.500	3.182	9.55	39.0
4	0.080	1.375	3.460	10.38	53.5
Length/diameter = 4					
2	0.010	3.00	3.140	12.56	6.1
2	0.025	2.25	2.522	10.09	7.3
2	0.035	2.00	2.348	9.39	7.9
2	0.040	1.875	2.254	9.01	7.8
2	0.050	1.75	2.206	8.82	8.8
2	0.060	1.625	2.150	8.60	9.3
2	0.075	1.50	2.140	8.56	10.8
2	0.090	1.375	2.124	8.49	12.0
2	0.115	1.250	2.232	8.93	16.3
2	0.140	1.125	2.386	9.55	22.2
2	0.145	1.125	2.482	9.93	25.5
3	0.0095	3.00	3.204	12.81	9.1
3	0.0100	3.00	3.214	12.86	9.7
3	0.030	2.00	2.468	9.87	11.4
3	0.045	1.75	2.412	9.65	14.5
3	0.055	1.625	2.422	9.69	16.9
3	0.065	1.50	2.430	9.72	19.1
3	0.080	1.375	2.558	10.23	25.3
3	0.095	1.250	2.638	10.95	34.1

General Electric Thermionic (continued) $^{244}Cm_2O_3$ – 1 kw_t – 1650°C

Stress rate safety factor	Allowable pressure rate, psi/hr	Capsule dimensions, in. i.d.	o.d.	length	Capsule wt, lb
Length/diameter = 4 (continued)					
4	0.010	3.00	3.286	13.15	13.3
4	0.030	2.00	2.646	10.58	17.4
4	0.035	1.875	2.608	10.43	18.6
4	0.050	1.625	2.654	10.61	25.0
4	0.060	1.500	2.766	11.06	31.7
4	0.070	1.375	2.916	11.67	40.6
4	0.080	1.250	3.146	12.58	54.6
Length/diameter = 5					
2	0.008	3.00	3.112	15.56	5.9
2	0.010	2.75	2.878	14.39	5.8
2	0.025	2.00	2.242	11.21	6.4
2	0.040	1.75	2.104	10.52	7.9
2	0.050	1.625	2.048	10.24	8.7
2	0.060	1.500	1.984	9.92	9.2
2	0.075	1.375	1.962	9.81	10.4
2	0.095	1.250	1.984	9.92	12.7
2	0.120	1.125	2.074	10.37	16.8
2	0.150	1.00	2.300	11.50	26.0
3	0.0075	3.00	3.160	15.80	8.7
3	0.0080	3.00	3.170	15.85	9.3
3	0.0100	2.75	2.846	14.73	9.2
3	0.0250	2.00	2.380	11.90	11.0
3	0.030	1.875	2.312	11.56	11.7
3	0.035	1.750	2.238	11.19	12.0
3	0.045	1.625	2.240	11.20	14.5
3	0.055	1.500	2.236	11.18	16.7
3	0.065	1.375	2.228	11.14	18.4
3	0.080	1.250	2.326	11.63	23.9
3	0.095	1.125	2.464	12.32	31.3
4	0.0080	3.00	3.226	16.13	12.7
4	0.0100	2.75	3.012	15.06	12.7
4	0.025	2.00	2.520	12.60	16.3
4	0.035	1.75	2.434	12.17	19.0
4	0.040	1.625	2.378	11.89	19.5
4	0.050	1.50	2.450	12.25	24.7
4	0.060	1.375	2.536	12.68	30.7
4	0.070	1.250	2.652	13.26	38.4
4	0.080	1.125	2.832	14.16	50.2

FOR Karl Haff.

AVZ = 3415 BTU/hr

75% $244Cm_2O_3$ in Fuel

25% void

	Rupture	1% Crp
SIGU	215,000	215,000
GAMMA	1.00	1.00
ALPHA	0.8188 E-06	0.2374 E-06
XM	0.5113 E-04	0.4860 E-04
XKO	0.1338 E+11	0.2194 E+10
RESIG	0.09289	0.8125

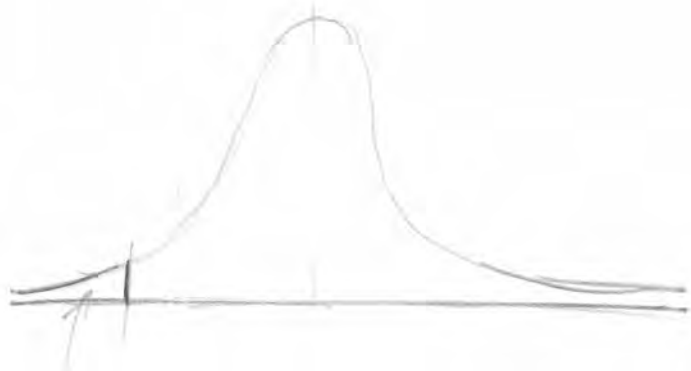

0.0001

Choose 0.0001 probability of rupture in 1 yr.

2.32 st. dev = 0.01

3.10 = 0.001

~ 3.74 = 0.0001

$$\sigma = \bar{\sigma}\left[1-(2.33)(.09289)\right]$$

$$\text{Safety Factor} = \frac{1}{1-(3.74)(.09289)} = \boxed{1.532}$$

8 calculations

$t \cong 10$

Rupture in 1 yr - SC = SU = 1.532

T = 3462 L/D = 3

T = " L/D = 4

T = 3822 L/D = 3

T = 3822 L/D = 4

1% Crp in 1 yr, Sc = Su = 1

T = 3462 L/D = 3

T = " L/D = 4

T = 3822 L/D = 3

T = 3822 L/D = 4

Fuel power = $(0.75)(26\ W/cm^3)(3.413\ \frac{BTU}{hr \cdot W})(16.387) = \underline{1091\ BTU/hr \cdot in^3}$

$k \cong 1$ BTU/hr ft °F ; $f(z) = (0.75)(10.7)\ g/cm^3\ \frac{16.387}{453.6\ g/\#} = 0.290$

$$\text{Lambda} = \frac{0.693}{(0.181\times10^2)(.8766\times10^4)} = 4.367\times10^{-6}$$

Table 1. Powder Metallurgy Tungsten Capsule Dimensions

Fuel loading — 1 kw, $^{244}Cm_2O_3$
Maximum wall temperature - 1850°C
Design life to rupture — 1 year

Stress rate safety factor	Pressure rate, psi/hr	Capsule dimensions, in. i.d.	o.d.	length	Total wt, lb
Length/diameter = 3					
4	0.020	2.5	~~2~~ 3.536	10.61	36.0
4	0.035	2.0	~~2~~ 3.898	11.70	68.4
3	0.015	3.0	3.625	10.88	25.1 0.3125
3	0.030	2.25	3.338	10.01	32.8
3	0.040	2.00	3.464	10.39	44.0
2	0.015	3.00	3.402	10.21	14.8
2	0.025	2.50	3.088	9.27	16.9
2	0.045	2.00	2.966	8.90	23.0
2	0.050	1.875	2.922	8.77	23.6
2	0.060	1.75	3.032	9.09	29.5
2	0.070	1.625	3.168	9.50	36.7
2	0.080	1.50	3.354	10.06	46.7
Length/diameter = 4					
4	0.010	3.00	3.550	14.20	28.4
4	0.035	1.75	3.412	13.65	61.8
3	0.010	3.00	3.402	13.61	19.5
3	0.030	2.00	2.966	11.87	30.8
3	0.035	1.875	2.998	11.99	35.2
3	0.040	1.75	3.032	12.12	39.6
2	0.025	2.25	2.78	11.12	16.4
2	0.040	1.875	2.652	10.61	20.3
2	0.045	1.75	2.596	10.38	20.6
2	0.055	1.625	2.666	10.67	25.5
2	0.065	1.50	2.752	11.0	31.1
2	0.075	1.375	2.862	11.45	38.0

Length/diameter = 5

4	0.008	3.00	3.430	17.15	26.4
4	0.010	2.75	3.254	16.27	27.2
4	0.030	1.75	3.032	15.16	49.8
4	0.035	1.625	3.168	15.84	62.3
3	0.0085	3.00	3.338	16.69	19.9
3	0.025	2.00	2.764	13.82	27.4
3	0.030	1.875	2.782	13.91	31.8
3	0.040	1.625	2.814	14.07	39.8
2	0.009	3.00	3.234	16.17	13.2
2	0.015	2.50	2.834	14.17	14.1
2	0.040	1.75	2.474	12.37	20.6
2	0.045	1.625	2.410	12.05	20.7
2	0.055	1.50	2.462	12.31	25.2
2	0.065	1.375	2.522	12.61	30.1

wall < $\frac{1}{4}$" $\frac{L}{D} = 3$; 1 kw capsule

$\sigma = 3$

1% in year - 3

rupture in yr. - 3

0.1% prob of failure in one year

1650 & 1850°C

3000 3360

6"

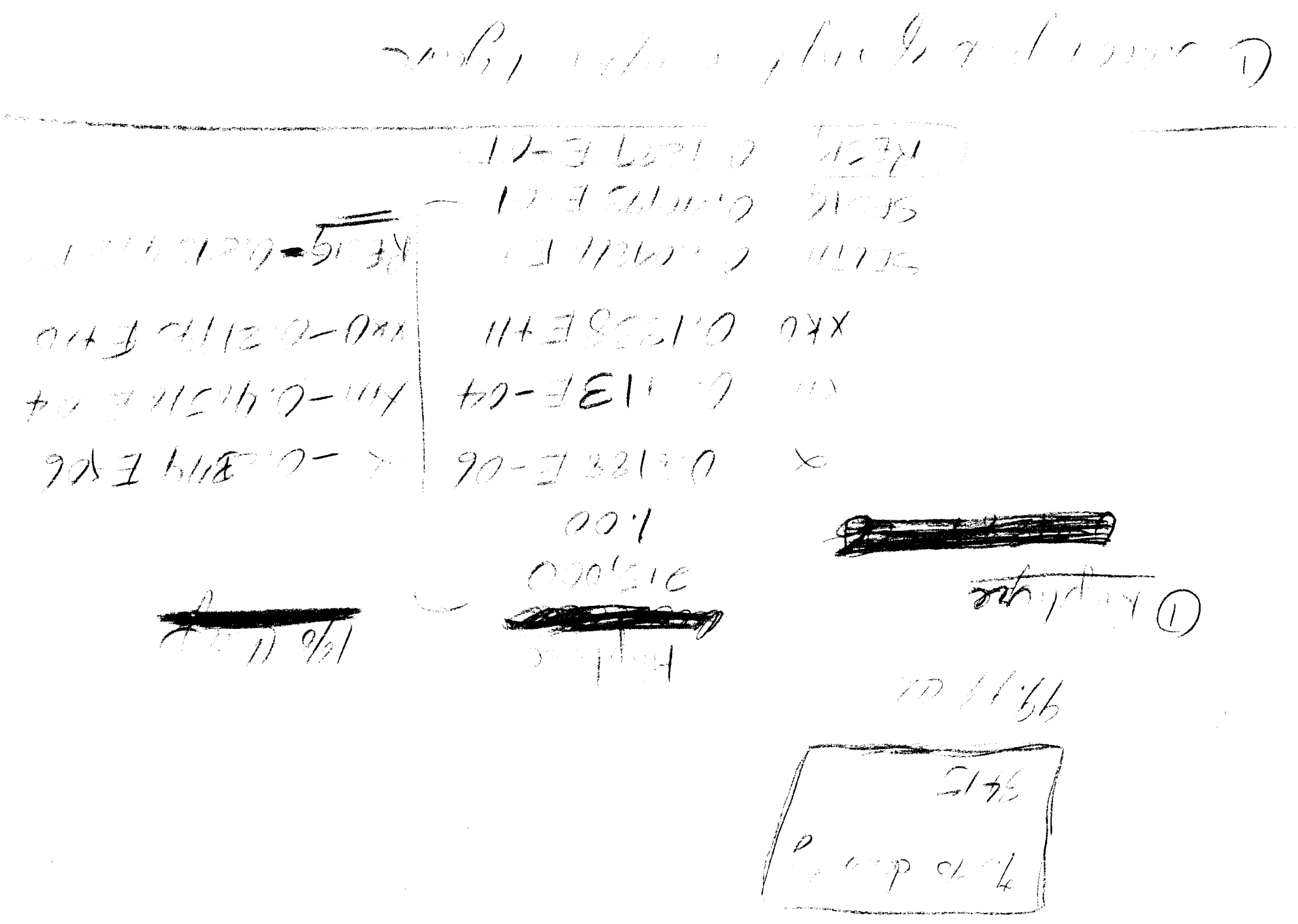

```
T8 = 3462.0      A =     1454.0      ETA =  0.4      BETA =  0.0
DELTA =  0.0          C =  1.00      G =  1.00      GAMMA = 1.00
RR =   18520.0      E =  1.000      PS =  0.0       TS =   1.0
H =        0.865      ZM =  244.0      TA = 3462.0      TA1 =     0.0
LAMBDA =     0.43680E-05      N =  50       NN =  50

MOPT =  3      NMAX =  6      NQ =  3

THE FOLLOWING THREE ROWS ARE THE CONTENTS OF THE X, P, AND XK ARRAYS

     0.0200      0.0         0.0200      0.0         0.0         0.0         0.0         0.0         0.0200
     0.6970      0.3860      0.6970      0.6970      0.0         0.0         0.0         0.0         0.6970
     0.0650      5.5400      5.5400      1.0000      1.0000      1.0000      1.0000      0.0400      1.0000

ALPHA =     0.81880E 06 -?
XM =     0.51130E-04
YK =     0.13380E 11
                 0.06                 1.5

X4U = 0.250      X4L = 0.600      R3U = 1.000      R3L = 0.250

SIGU =   215000.      SC = 3.00      SU = 3.00      PHI =  0.10E-03
Q =  0.10E-03      DELRO =  0.10E-03      DELX2 =  0.10E-03      DELX4 =  0.10E-04
TAU =  0.0            T81 =   3462.      T82 =      1.      XLD =   3.0
RO = 0.610      X(2) = 0.100      X(4) = 0.250      THETA =  0.8766E 04

IX =   2      NLAM =   0      NITER =   0      ITER =  20      LMOST =   0
G = 0.990      C = 1.000      CRIT = 1.00000      ALAM = 0.0

   M=      1   D=  0.324600E 01   W=  0.244186E 03   YSQ=  0.621916E 06   Z=  0.621916E 06   LSTOP=      0

    0.776076E 03     0.630247E-01

    0.140060E 03     0.250000E 00

   -0.224600E 01     0.0

RADII ARE   1.03475   1.05475   1.11777   1.13777   1.38777   1.38777   1.38777   1.38777   1.38777
L = 0.83266E 01   AV2 = 0.34129E 04   W1 = 0.14768E 03   W2 = 0.53206E 02   W3 = 0.24418E 03   WT = 0.13977E 02

   M=      2   D=  0.156967E 01   W=  0.222233E 03   YSQ=  0.165826E 06   Z=  0.165826E 06   LSTOP=      0

   -0.321570E 03     0.562373E-01

    0.249836E 03     0.250012E 00

   -0.569668E 00     0.168071E 02

RADII ARE   1.10795   1.12795   1.18419   1.20419   1.45420   1.45420   1.45420   1.45420   1.45420
L = 0.87252E 01   AV2 = 0.34127E 04   W1 = 0.13448E 03   W2 = 0.46240E 02   W3 = 0.22223E 03   WT = 0.15356E 02

   M=      3   D=  0.107993E 01   W=  0.211497E 03   YSQ=  0.115849E 05   Z=  0.115849E 05   LSTOP=      0

   -0.996631E 02     0.529863E-01

    0.406472E 02     0.249917E 00

   -0.799255E-01     0.253847E 02

RADII ARE   1.14763   1.16763   1.22061   1.24061   1.49053   1.49053   1.49053   1.49053   1.49053
```

```
L = 0.89832E 01   AV2 = 0.34126E 04   W1 = 0.12806E 03   W2 = 0.42936E 02   W3 = 0.21150E 03   WT = 0.16136E 02

   M=      4   D=  0.100280E 01   W=  0.209410E 03   YSQ=  0.643875E 05   Z=  0.643875E 05   LSTOP=      0
    0.134206E 03     0.523654E-01

    0.215351E 03     0.249915E 00

   -0.280190E-02     0.290876E 02

RADII ARE   1.15555   1.17555   1.22791   1.24791   1.49783   1.49783   1.49783   1.49783   1.49783
L = 0.89870E 01   AV2 = 0.34123E 04   W1 = 0.12675E 03   W2 = 0.42311E 02   W3 = 0.20941E 03   WT = 0.16295E 02

   M=      5   D=  0.999883E 00   W=  0.209328E 03   YSQ=  0.193571E 05   Z=  0.193571E 05   LSTOP=      0

   -0.366919E 01     0.523404E-01

    0.139082E 03     0.249905E 00

    0.117242E-03     0.280201E 02

RADII ARE   1.15580   1.17580   1.22814   1.24814   1.49804   1.49804   1.49804   1.49804   1.49804
L = 0.89883E 01   AV2 = 0.34119E 04   W1 = 0.12670E 03   W2 = 0.42287E 02   W3 = 0.20933E 03   WT = 0.16299E 02

   M=      6   D=  0.100015E 01   W=  0.209333E 03   YSQ=  0.560565E 04   Z=  0.560565E 04   LSTOP=      0

   -0.334497E 01     0.523407E-01

    0.747961E 02     0.249901E 00

   -0.149727E-03     0.280579E 02

RADII ARE   1.15575   1.17575   1.22809   1.24809   1.49799   1.49799   1.49799   1.49799   1.49799
L = 0.89880E 01   AV2 = 0.34117E 04   W1 = 0.12670E 03   W2 = 0.42290E 02   W3 = 0.20933E 03   WT = 0.16298E 02

   M=      7   D=  0.100004E 01   W=  0.209329E 03   YSQ=  0.248670E 05   Z=  0.248670E 05   LSTOP=      0

    0.562256E 01     0.523389E-01

    0.157593E 03     0.249898E 00

   -0.381470E-04     0.280998E 02

RADII ARE   1.15574   1.17574   1.22808   1.24808   1.49798   1.49798   1.49798   1.49798   1.49798
L = 0.89879E 01   AV2 = 0.34115E 04   W1 = 0.12669E 03   W2 = 0.42288E 02   W3 = 0.20933E 03   WT = 0.16298E 02

   M=      8   D=  0.100014E 01   W=  0.209316E 03   YSQ=  0.335985E 05   Z=  0.335985E 05   LSTOP=      0

    0.265964E 02     0.523511E-01

    0.181359E 03     0.249968E 00

   -0.140190E-03     0.282899E 02

RADII ARE   1.15550   1.17550   1.22785   1.24785   1.49782   1.49782   1.49782   1.49782   1.49782
L = 0.89869E 01   AV2 = 0.34113E 04   W1 = 0.12671E 03   W2 = 0.42299E 02   W3 = 0.20932E 03   WT = 0.16297E 02

   M=      9   D=  0.999951E 00   W=  0.209311E 03   YSQ=  0.424148E 05   Z=  0.424148E 05   LSTOP=      0

    0.213379E 00     0.523487E-01

    0.205948E 03     0.249960E 00

    0.488758E-04     0.280884E 02

RADII ARE   1.15546   1.17546   1.22781   1.24780   1.49776   1.49776   1.49776   1.49776   1.49776
```

```
L = 0.89866E 01   AV2 = 0.34109E 04   W1 = 0.12670E 03   W2 = 0.42293E 02   W3 = 0.20931E 03   WT = 0.16296E 02

   M=    10   D=  0.100013E 01   W=  0.209313E 03   YSQ=  0.582041E 05   Z=  0.582041E 05   LSTOP=     0

   -0.104756E 02     0.523484E-01

    0.241028E 03     0.249956E 00

   -0.133514E-03     0.280648E 02

RADII ARE   1.15543   1.17543   1.22778   1.24778   1.49774   1.49774   1.49774   1.49774   1.49774
L = 0.89864E 01   AV2 = 0.34107E 04   W1 = 0.12670E 03   W2 = 0.42298E 02   W3 = 0.20931E 03   WT = 0.16295E 02

   M=    11   D=  0.100001E 01   W=  0.209311E 03   YSQ=  0.156984E 05   Z=  0.156984E 05   LSTOP=     0

    0.166741E 02     0.523446E-01

    0.124179E 03     0.249939E 00

   -0.572205E-05     0.281463E 02

RADII ARE   1.15545   1.17545   1.22779   1.24779   1.49773   1.49773   1.49773   1.49773   1.49773
L = 0.89864E 01   AV2 = 0.34105E 04   W1 = 0.12670E 03   W2 = 0.42296E 02   W3 = 0.20931E 03   WT = 0.16294E 02

   M=    12   D=  0.100013E 01   W=  0.209306E 03   YSQ=  0.457798E 05   Z=  0.457798E 05   LSTOP=     0

    0.214062E 01     0.523512E-01

    0.213951E 03     0.249975E 00

   -0.126839E-03     0.280301E 02

RADII ARE   1.15532   1.17532   1.22767   1.24767   1.49765   1.49765   1.49765   1.49765   1.49765
L = 0.89859E 01   AV2 = 0.34103E 04   W1 = 0.12671E 03   W2 = 0.42302E 02   W3 = 0.20931E 03   WT = 0.16293E 02

   M=    13   D=  0.100003E 01   W=  0.209299E 03   YSQ=  0.310570E 05   Z=  0.310570E 05   LSTOP=     0

   -0.316577E 01     0.523529E-01

    0.176201E 03     0.249993E 00

   -0.286102E-04     0.280786E 02

RADII ARE   1.15526   1.17526   1.22761   1.24761   1.49760   1.49760   1.49760   1.49760   1.49760
L = 0.89856E 01   AV2 = 0.34102E 04   W1 = 0.12671E 03   W2 = 0.42303E 02   W3 = 0.20930E 03   WT = 0.16293E 02

   M=    14   D=  0.100004E 01   W=  0.209302E 03   YSQ=  0.890287E 05   Z=  0.890287E 05   LSTOP=     0

    0.431006E 01     0.523504E-01

    0.298346E 03     0.249976E 00

   -0.448227E-04     0.280773E 02

RADII ARE   1.15526   1.17526   1.22761   1.24761   1.49759   1.49759   1.49759   1.49759   1.49759
L = 0.89855E 01   AV2 = 0.34099E 04   W1 = 0.12670E 03   W2 = 0.42302E 02   W3 = 0.20930E 03   WT = 0.16292E 02

   M=    15   D=  0.100007E 01   W=  0.209304E 03   YSQ=  0.213018E 05   Z=  0.213018E 05   LSTOP=     0

    0.198967E 02     0.523473E-01

    0.144589E 03     0.249957E 00
```

```
-0.734329E-04     0.280792E 02

RADII ARE   1.15526   1.17526   1.22760   1.24760   1.49756   1.49756   1.49756   1.49756   1.49756
L = 0.89854E 01   AV2 = 0.34097E 04   W1 = 0.12670E 03   W2 = 0.42301E 02   W3 = 0.20930E 03   WT = 0.16291E 02

M=    16   D=  0.100003E 01   W=  0.209297E 03   YSQ=  0.737510E 04   Z=  0.737510E 04   LSTOP=     0

-0.236189E 02     0.523495E-01

 0.825667E 02     0.249974E 00

-0.314713E-04     0.278646E 02

RADII ARE   1.15517   1.17517   1.22752   1.24752   1.49749   1.49749   1.49749   1.49749   1.49749
L = 0.89849E 01   AV2 = 0.34094E 04   W1 = 0.12670E 03   W2 = 0.42303E 02   W3 = 0.20930E 03   WT = 0.16290E 02

M=    17   D=  0.999997E 00   W=  0.209295E 03   YSQ=  0.740425E 04   Z=  0.740425E 04   LSTOP=     0

 0.633789E 01     0.523486E-01

 0.858142E 02     0.249971E 00

 0.339746E-05     0.280854E 02

RADII ARE   1.15512   1.17512   1.22747   1.24747   1.49744   1.49744   1.49744   1.49744   1.49744
L = 0.89846E 01   AV2 = 0.34091E 04   W1 = 0.12669E 03   W2 = 0.42303E 02   W3 = 0.20929E 03   WT = 0.16288E 02

M=    18   D=  0.100000E 01   W=  0.209293E 03   YSQ=  0.365882E 05   Z=  0.365882E 05   LSTOP=     0

-0.102502E 02     0.523481E-01

 0.191006E 03     0.249967E 00

-0.286102E-05     0.280143E 02

RADII ARE   1.15507   1.17507   1.22741   1.24741   1.49738   1.49738   1.49738   1.49738   1.49738
L = 0.89843E 01   AV2 = 0.34087E 04   W1 = 0.12669E 03   W2 = 0.42304E 02   W3 = 0.20929E 03   WT = 0.16287E 02

M=    19   D=  0.100009E 01   W=  0.209295E 03   YSQ=  0.838666E 05   Z=  0.838666E 05   LSTOP=     0

 0.676733E 01     0.523463E-01

 0.289518E 03     0.249956E 00

-0.886917E-04     0.280344E 02

RADII ARE   1.15504   1.17504   1.22739   1.24739   1.49734   1.49734   1.49734   1.49734   1.49734
L = 0.89841E 01   AV2 = 0.34084E 04   W1 = 0.12669E 03   W2 = 0.42304E 02   W3 = 0.20929E 03   WT = 0.16285E 02

M=    20   D=  0.999952E 00   W=  0.209290E 03   YSQ=  0.195199E 05   Z=  0.195199E 05   LSTOP=     0

-0.172576E 02     0.523441E-01

 0.138644E 03     0.249947E 00

 0.481009E-04     0.280139E 02

RADII ARE   1.15499   1.17499   1.22733   1.24733   1.49728   1.49728   1.49728   1.49728   1.49728
L = 0.89837E 01   AV2 = 0.34079E 04   W1 = 0.12668E 03   W2 = 0.42303E 02   W3 = 0.20929E 03   WT = 0.16283E 02

M=    21   D=  0.100007E 01   W=  0.209290E 03   YSQ=  0.463880E 05   Z=  0.463880E 05   LSTOP=     0
```

```
    0.168801E 02     0.523440E-01

    0.214716E 03     0.249943E 00

   -0.724792E-04     0.281613E 02

RADII ARE   1.15491   1.17491   1.22725   1.24725   1.49719   1.49719   1.49719   1.49719   1.49719
L = 0.89831E 01   AV2 = 0.34075E 04   W1 = 0.12668E 03   W2 = 0.42305E 02   W3 = 0.20929E 03   WT = 0.16281E 02

RADII ARE   1.15489   1.17489   1.27472   1.29472   1.89472   1.89472   1.89472   1.89472   1.89472
L = 0.89831E 01   AV2 = 0.34074E 04   W1 = 0.12668E 03   W2 = 0.42305E 02   W3 = 0.20929E 03   WT = 0.16281E 02
```
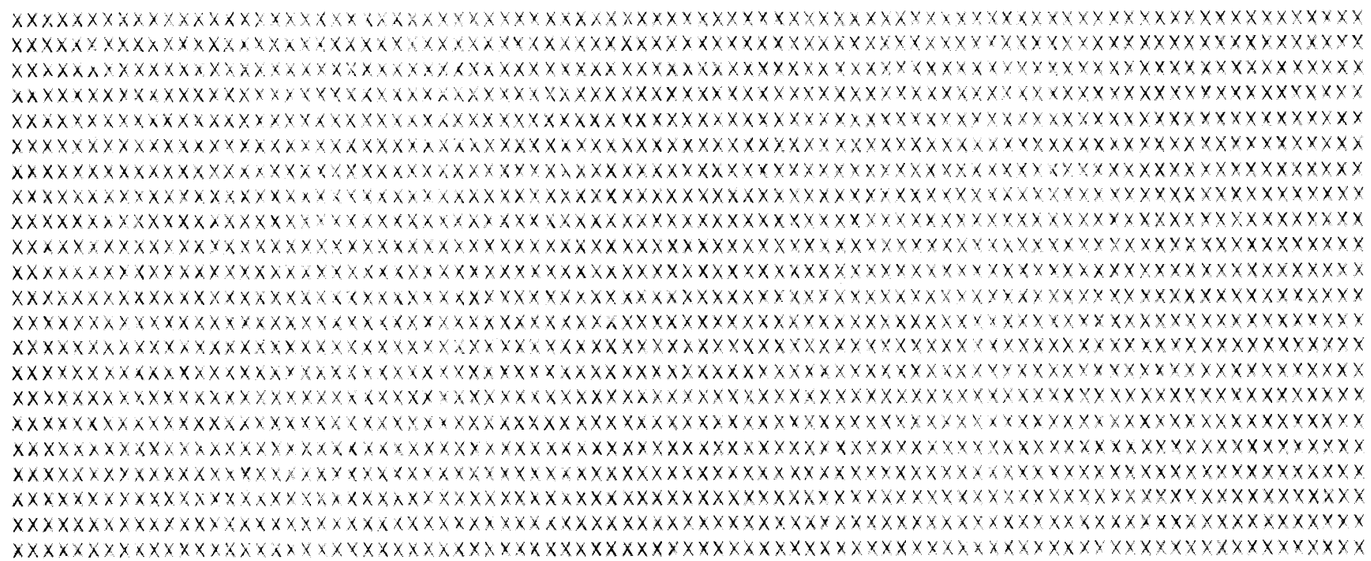
```
IEF285I   TMPWBG                                    PASSED
IEF285I   VOL SER NOS= AAA111.
IEF285I   SYSOUT                                    SYSOUT
IEF285I   VOL SER NOS=        .
IEF285I   LABLIB                                    KEPT
IEF285I   VOL SER NOS= AAA111.
IEF285I   UT20                                      KEPT
IEF285I   VOL SER NOS= 222222.
IEF285I   UT30                                      KEPT
IEF285I   VOL SER NOS= 333333.
IEF285I   TMPWBG                                    KEPT
IEF285I   VOL SER NOS= AAA111.
     K10       CHARGE 11917    DATE 06-16-67        000 HOURS  02 MINUTES  30 SECONDS
```